EVOLUTION OF NEUTRON STARS IN NON-INTERACTING LOW-MASS BINARIES

SERGEI POPOV, MARINA AFONINA (SAI MSU)

2404.17549
2409.00714
2501.15918
2509.03001

VARIETY OF BINARY SYSTEMS

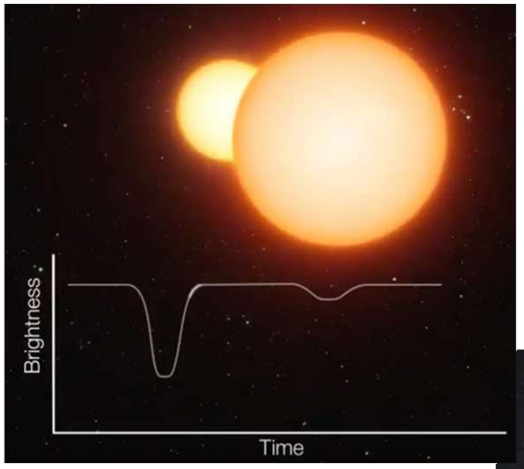

Eclipsing binaries

Visual binaries

Accreting binaries

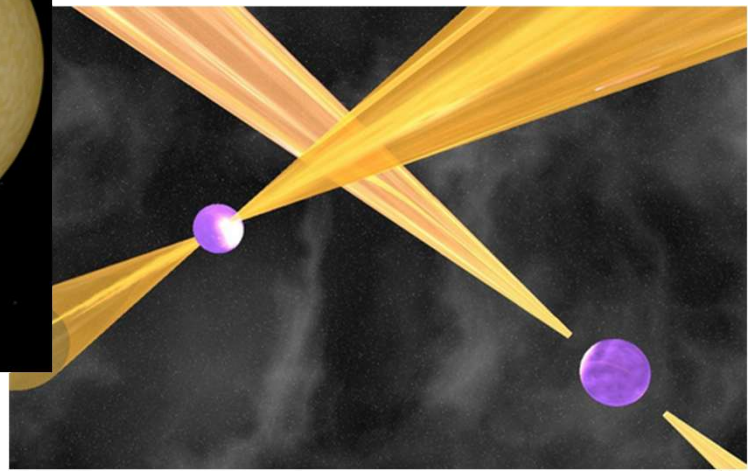

Relativistic binaries

FRACTION OF BINARIES

Mostly, massive stars at birth are members of binary or multiple systems.

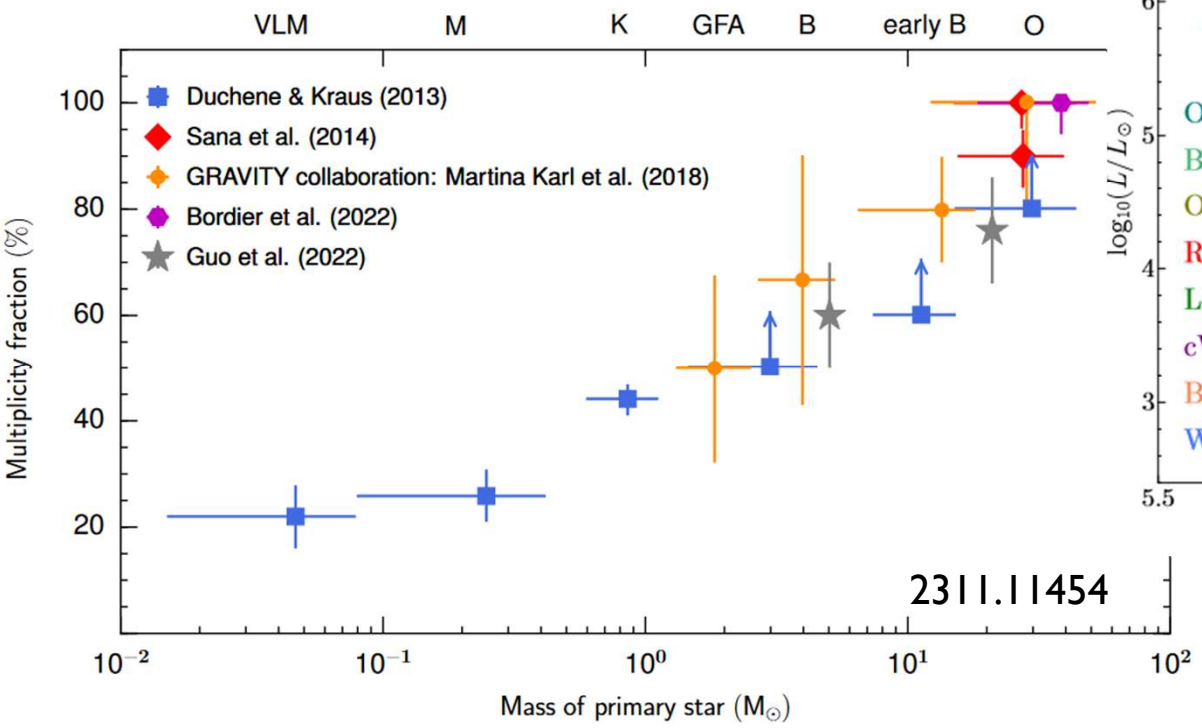

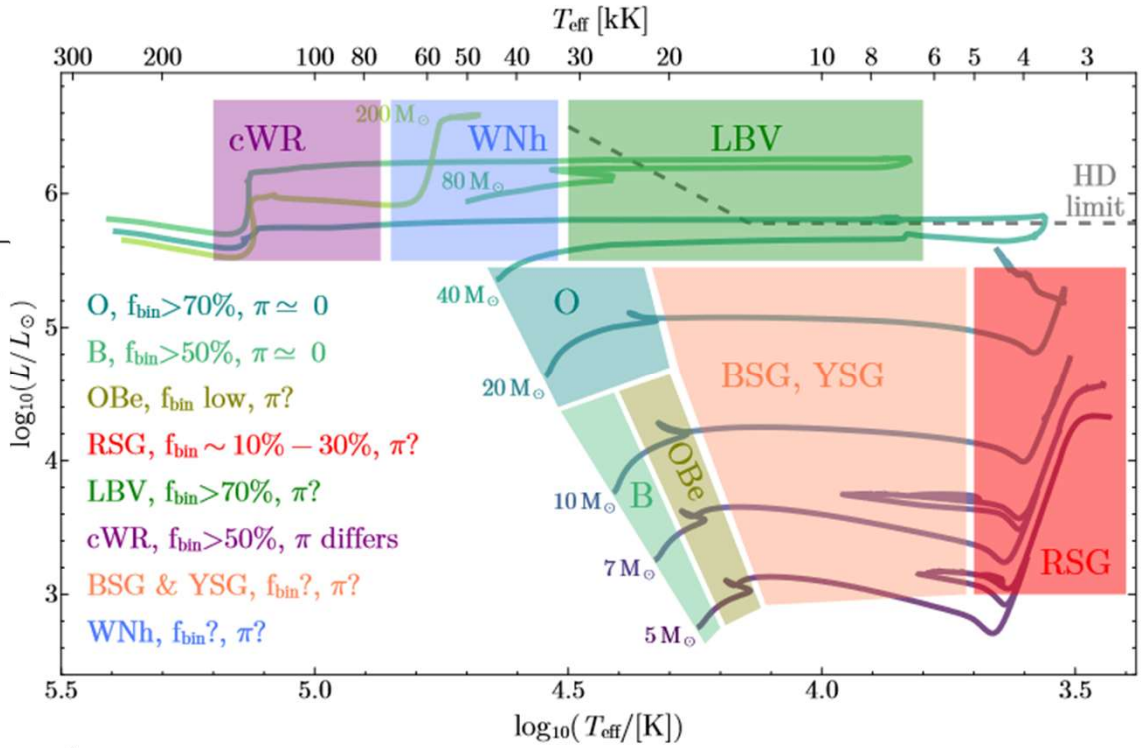

$$f(\log \mathrm{P[days]}) \sim (\log \mathrm{P})^{\pi}$$

OTHER MULTIPLES ARE ALSO IMPORTANT!

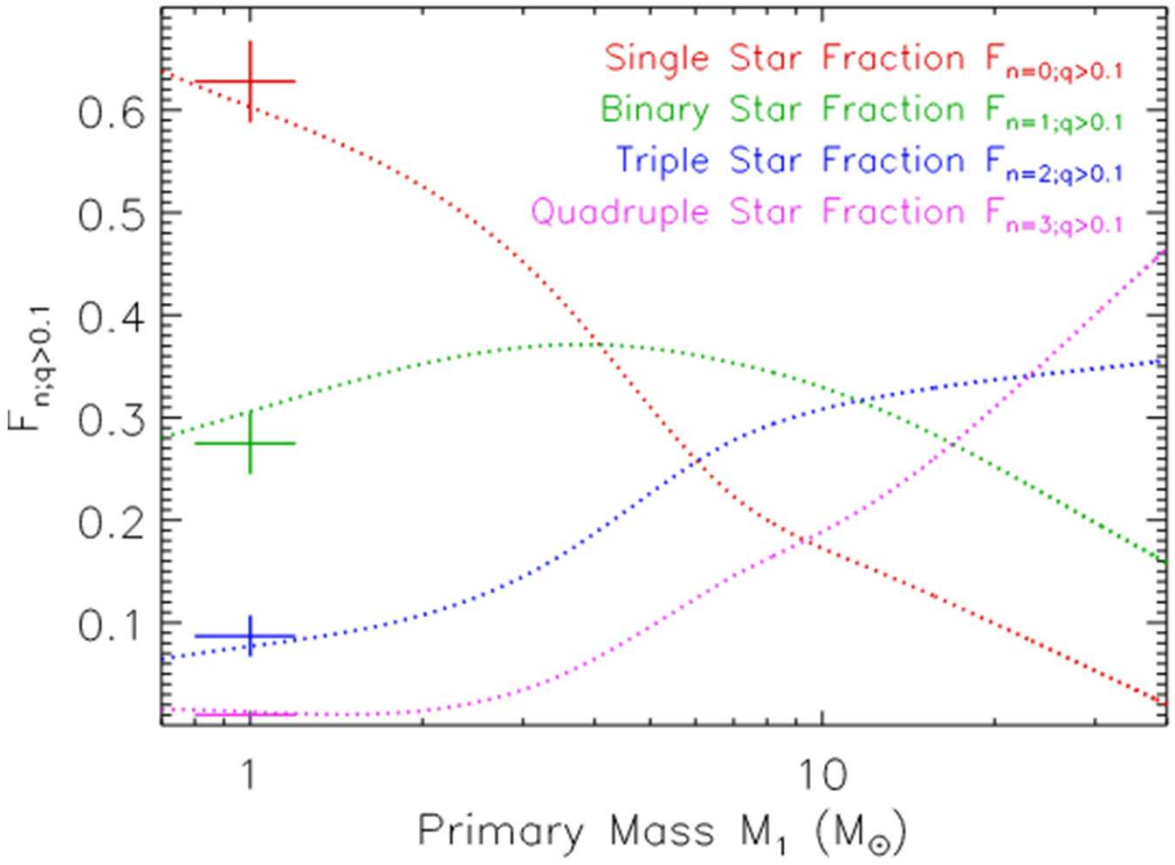

1606.05347

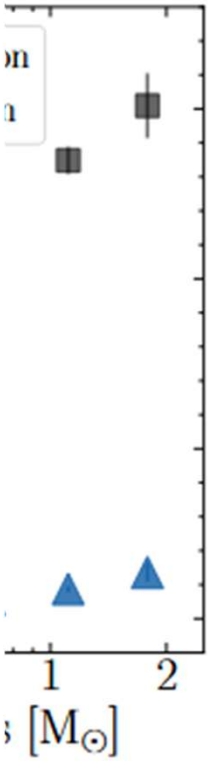

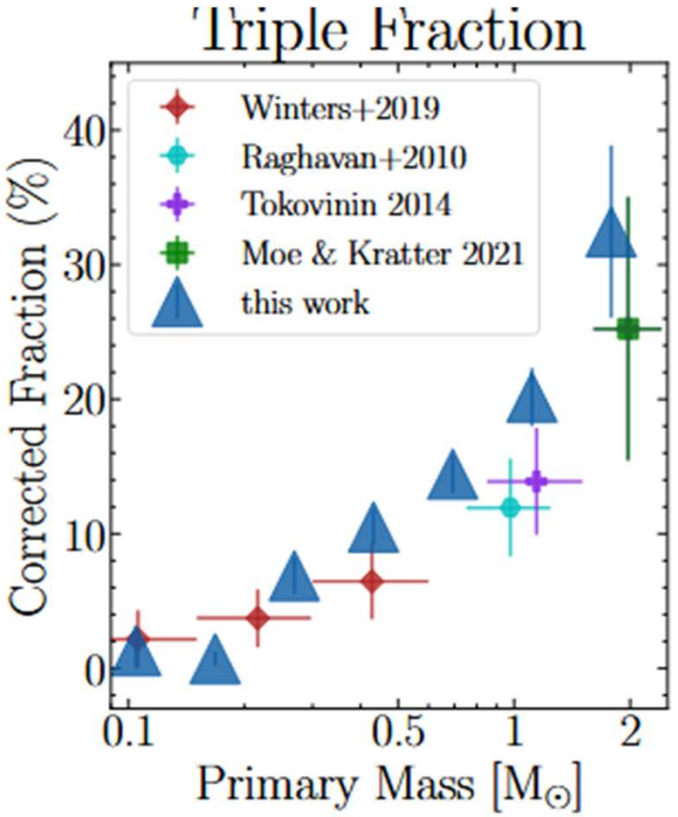

2506.16513

CLOSE BINARIES WITH ACCRETING COMPACT OBJECTS

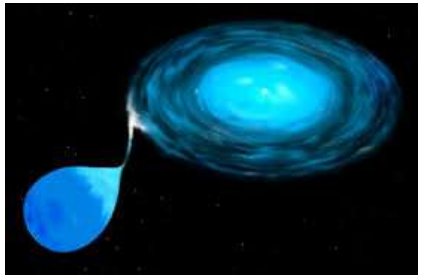

LMXBs
Roche lobe overflow.
Very compact systems.
Rapid NS rotation.
Produce mPSRs.

IMXBs
Very rare.
Roche lobe overflow.
Produce LMXBs(?)

HMXBs
Accretion from
the stellar wind.
Mainly Be/X-ray.
Wide systems.
Long NS spin periods.
Produce DNS.

Among binaries ~40% are close and ~96% are low and intermediate mass

Not in all binaries accretion is possible. A compact object spends just a fraction of its life as an accretor

LOW MASS X-RAY BINARIES

NSs as accretors
X-ray pulsars
Millisecond X-ray pulsars
Bursters
Atoll sources
Z-type sources

WDs as accretors
Cataclysmic variables
- Novae
- Dwarf novae
- Polars
- Intermediate polars

Supersoft sources (SSS)

BHs as accretors
X-ray novae
Microquasars
Massive X-ray binaries

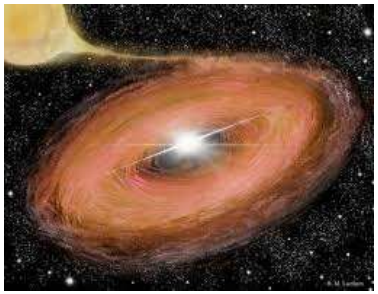

See a catalogue in 2303.16168

VARIOUS METHODS TO STUDY BINARY SYSTEMS

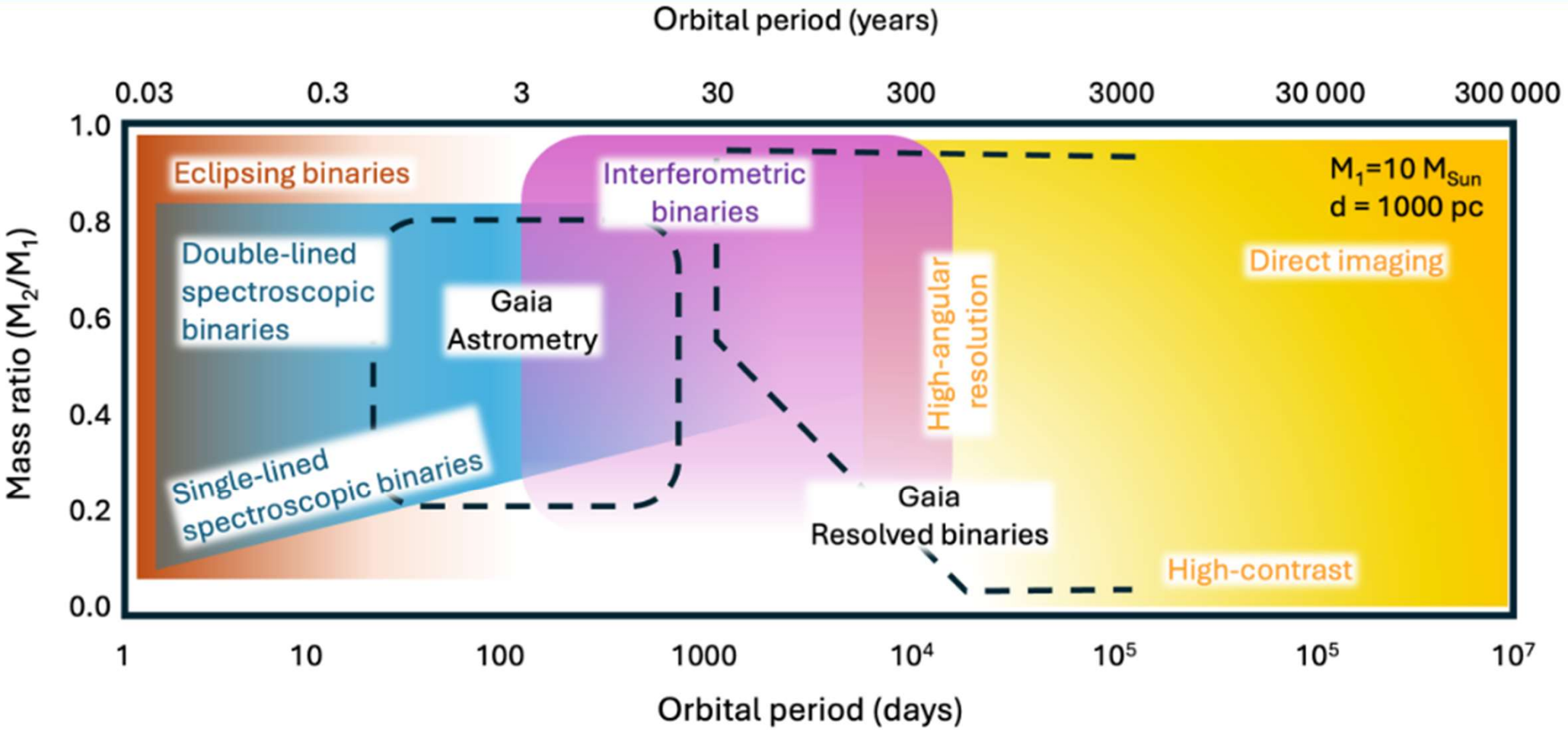

2504.00548

HOW TO FIND AN INVISIBLE OBJECT?

Astrometric binaries

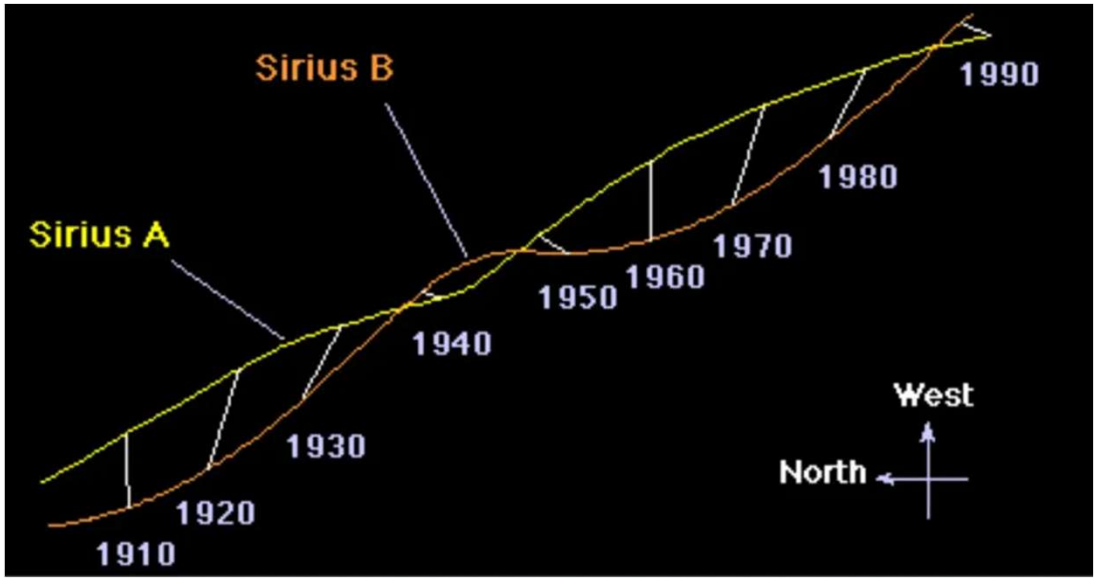

White dwarfs have been found as invisible massive companions already in the 19th century.

Spectroscopic binaries

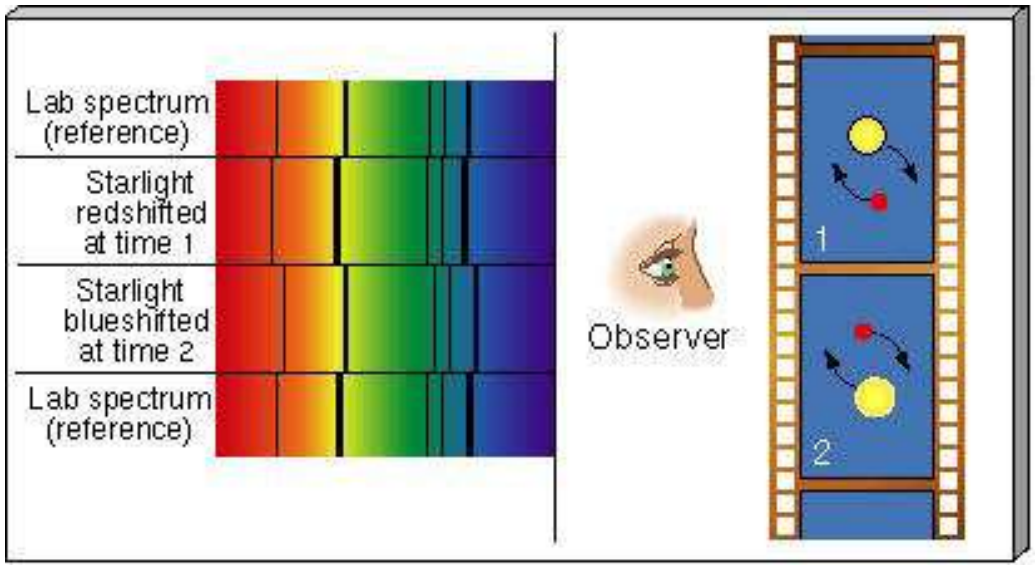

In 1966 Guseinov and Zeldovich proposed that non-accreting black holes can be found in such systems.

NON-INTERACTING BINARIES FOUND BY GAIA

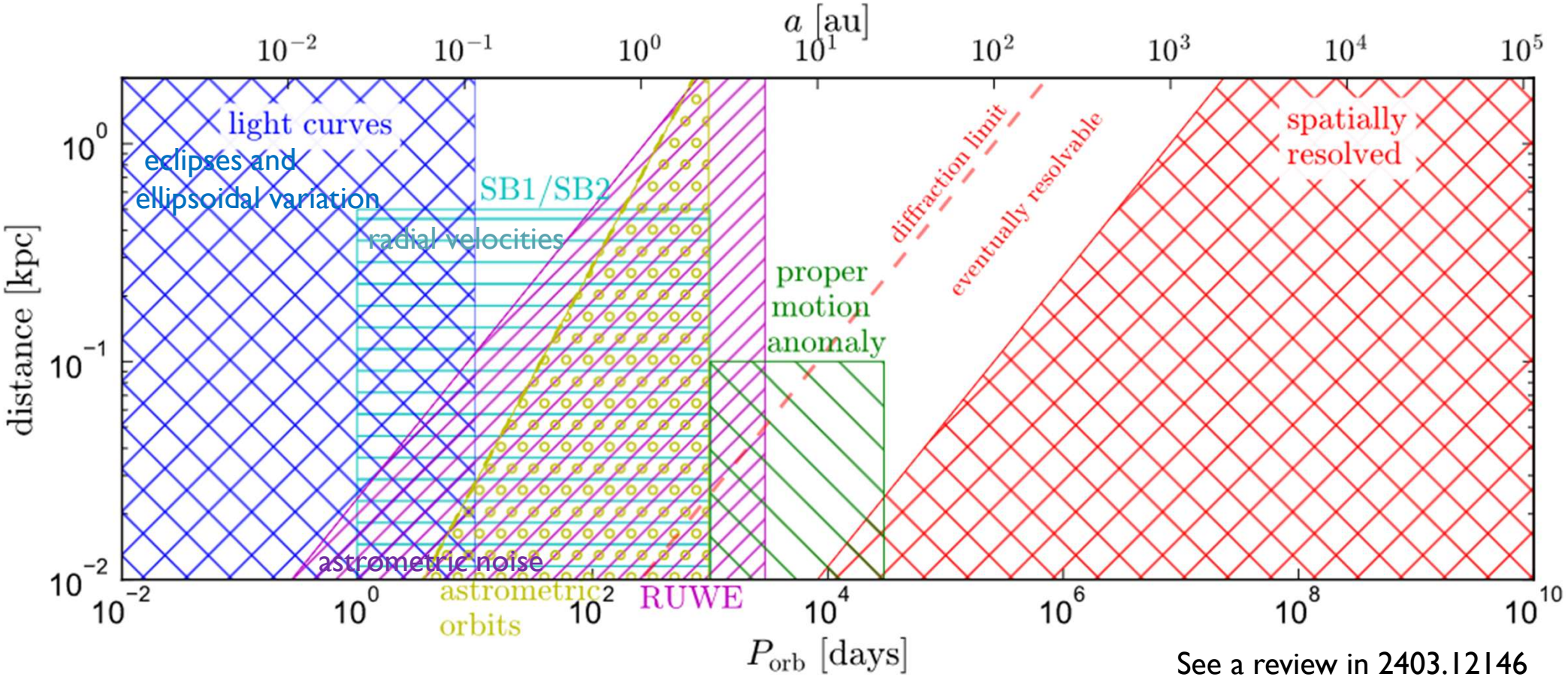

See a review in 2403.12146

BLACK HOLE BINARIES

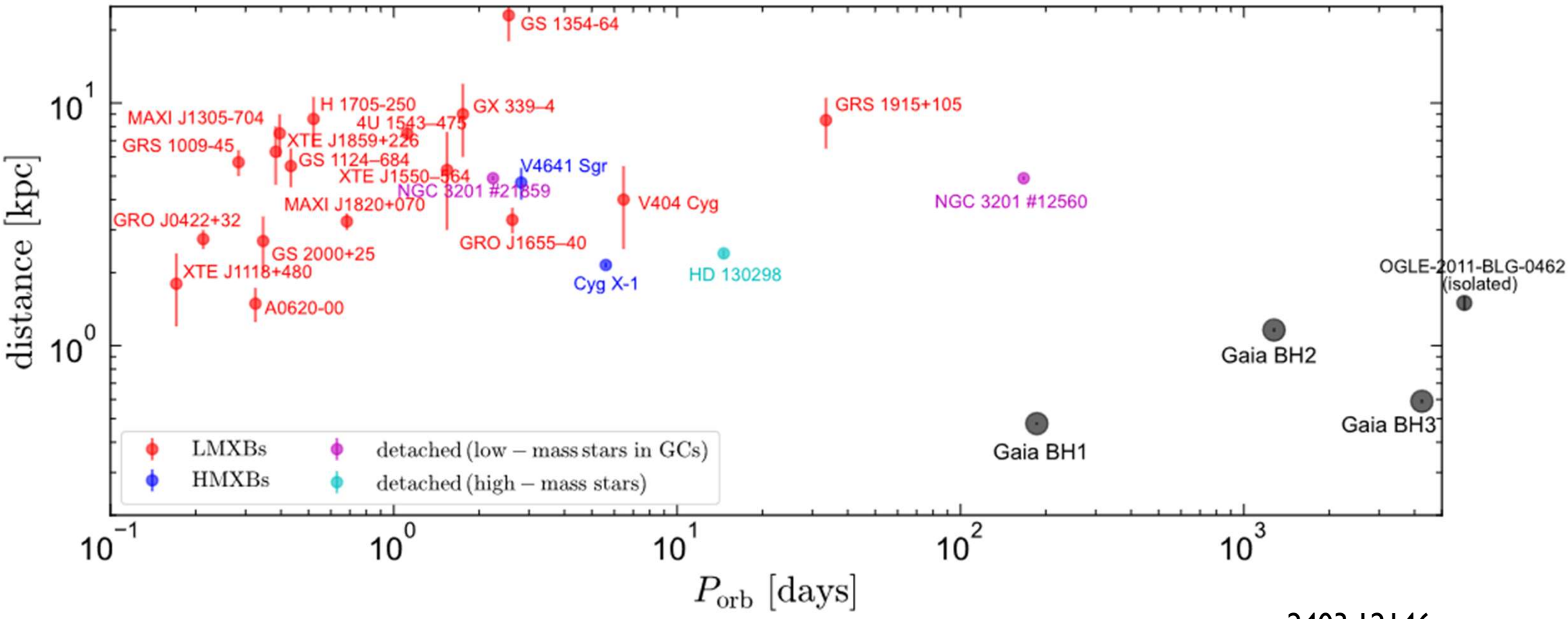

2403.12146

NEUTRON STAR BINARIES. I.

Name	$P_{\rm orb}$ [days]	$M_\star$ [$M_\odot$]	M_2 [$M_\odot$]	eccentricity	ϖ [mas]	G [mag]	$N_{\rm RVs}$
J0553-1349	189.10 ± 0.05	0.98 ± 0.06	1.33 ± 0.05	0.3879 ± 0.0007	2.505 ± 0.015	13.00	20
J2057-4742	230.15 ± 0.07	1.048 ± 0.031	1.31 ± 0.04	0.3095 ± 0.0026	1.745 ± 0.019	13.58	11
J1553-6846	310.17 ± 0.11	1.04 ± 0.05	1.323 ± 0.032	0.5314 ± 0.0021	1.344 ± 0.012	14.19	16
J2102+3703	481.04 ± 0.26	1.03 ± 0.03	1.473 ± 0.034	0.448 ± 0.009	1.521 ± 0.013	13.70	10
J0742-4749	497.6 ± 0.4	0.90 ± 0.05	1.28 ± 0.04	0.168 ± 0.004	1.035 ± 0.014	14.60	8
J0152-2049	536.14 ± 0.18	0.782 ± 0.03	1.291 ± 0.024	0.6615 ± 0.0010	2.453 ± 0.017	12.05	15
J0003-5604	561.83 ± 0.29	0.802 ± 0.03	1.34 ± 0.04	0.795 ± 0.005	2.183 ± 0.016	14.48	12
J1733+5808	570.94 ± 0.31	1.16 ± 0.05	1.362 ± 0.030	0.3093 ± 0.0010	1.452 ± 0.010	13.65	13
J1150-2203	631.81 ± 0.22	1.18 ± 0.06	1.39 ± 0.04	0.552 ± 0.004	1.738 ± 0.016	12.66	20
J1449+6919	632.65 ± 0.21	0.91 ± 0.05	1.258 ± 0.032	0.2668 ± 0.0010	1.812 ± 0.010	13.20	19
J0217-7541	636.1 ± 0.7	0.996 ± 0.033	1.396 ± 0.033	0.3228 ± 0.0033	1.193 ± 0.012	14.01	10
J0639-3655	654.6 ± 0.6	1.32 ± 0.06	1.70 ± 0.07	0.721 ± 0.013	1.130 ± 0.011	13.36	10
J1739+4502	657.4 ± 0.6	0.781 ± 0.03	1.38 ± 0.04	0.6777 ± 0.0018	1.126 ± 0.013	13.52	18
J0036-0932	719.8 ± 0.9	0.94 ± 0.04	1.362 ± 0.034	0.3993 ± 0.0021	1.661 ± 0.019	13.02	16
J1432-1021	730.9 ± 0.5	0.79 ± 0.03	1.898 ± 0.030	0.1203 ± 0.0022	1.367 ± 0.011	13.34	34
J1048+6547	827 ± 5	0.99 ± 0.05	1.52 ± 0.07	0.357 ± 0.009	0.916 ± 0.016	14.52	9
J2145+2837	889.5 ± 0.7	0.95 ± 0.05	1.396 ± 0.035	0.5840 ± 0.0035	4.137 ± 0.016	12.19	11
J2244-2236	938.3 ± 0.5	1.002 ± 0.03	1.443 ± 0.023	0.5666 ± 0.0011	2.079 ± 0.019	13.35	13
J0824+5254	1026.7 ± 3.3	1.102 ± 0.03	1.604 ± 0.034	0.686 ± 0.012	1.643 ± 0.015	13.59	13
J0230+5950	1029 ± 5	1.114 ± 0.03	1.401 ± 0.034	0.753 ± 0.011	2.523 ± 0.015	13.09	15
J0634+6256	1046.0 ± 2.1	1.18 ± 0.06	1.48 ± 0.09	0.564 ± 0.011	0.689 ± 0.019	14.62	10

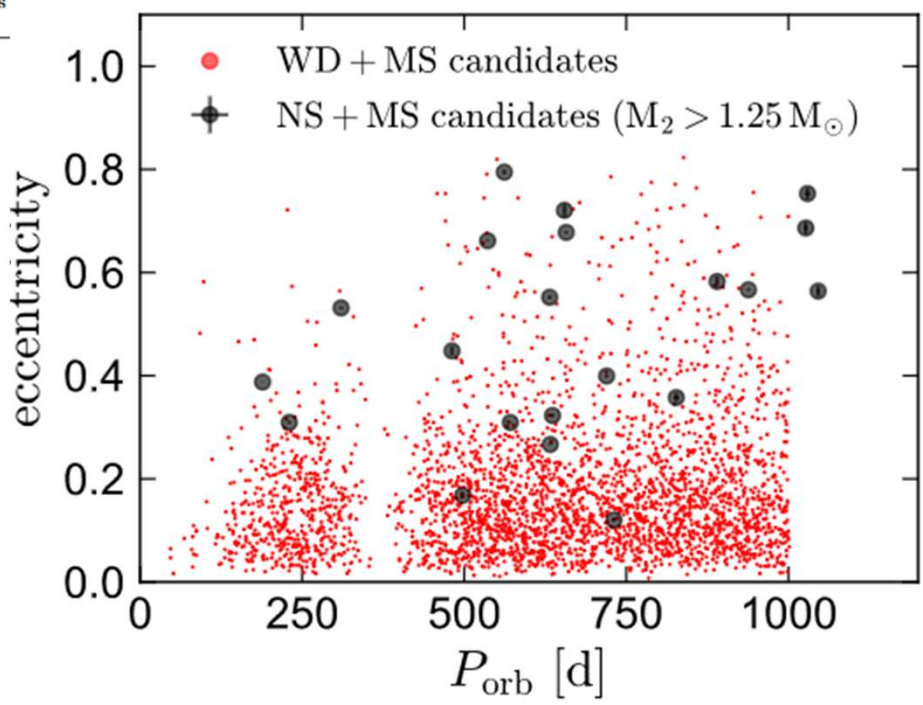

2405.00089

NEUTRON STAR BINARIES. II. X-RAY OBSERVATIONS

Source Name	distance pc	period[1] d	eccentricity	m_1[2] $M_\odot$	Type[3]	G mag	m_2[4] $M_\odot$
0616+2319	1111±30	$0.866605 \pm 1.0 \cdot 10^{-6}$	$0.0007^{+0.007}_{-0.0005}$	1.7±0.1	G7	13.21	1.1-1.3
1220+5841	219±3	927±11	0.52±0.01	0.70±0.2	K5	14.51	$1.43^{+0.16}_{-0.17}$
1313+4152	248±7	328±2	0.37±0.04	0.69±0.2	K7	16.18	$1.44^{+0.19}_{-0.20}$
1527+3536	118±0.9	$0.2556698 \pm 2 \cdot 10^{-7}$	0.0[5]	0.62±0.01	K9–M0	13.05	0.98±0.03
1832–0119	181±2	545±2	0.44±0.05	0.63-1.00	M2	15.62	1.44±0.17
2128+3316	227±2	1430±66	0.59±0.02	0.70±0.2	K5	14.87	$1.62^{+0.17}_{-0.18}$

Short period binaries are found in LAMOST radial velocity observations.

X-ray and UV observations.

Only 1527+3536 was detected in X-rays

2404.16170

MORE CANDIDATES (NSS AND WDS)

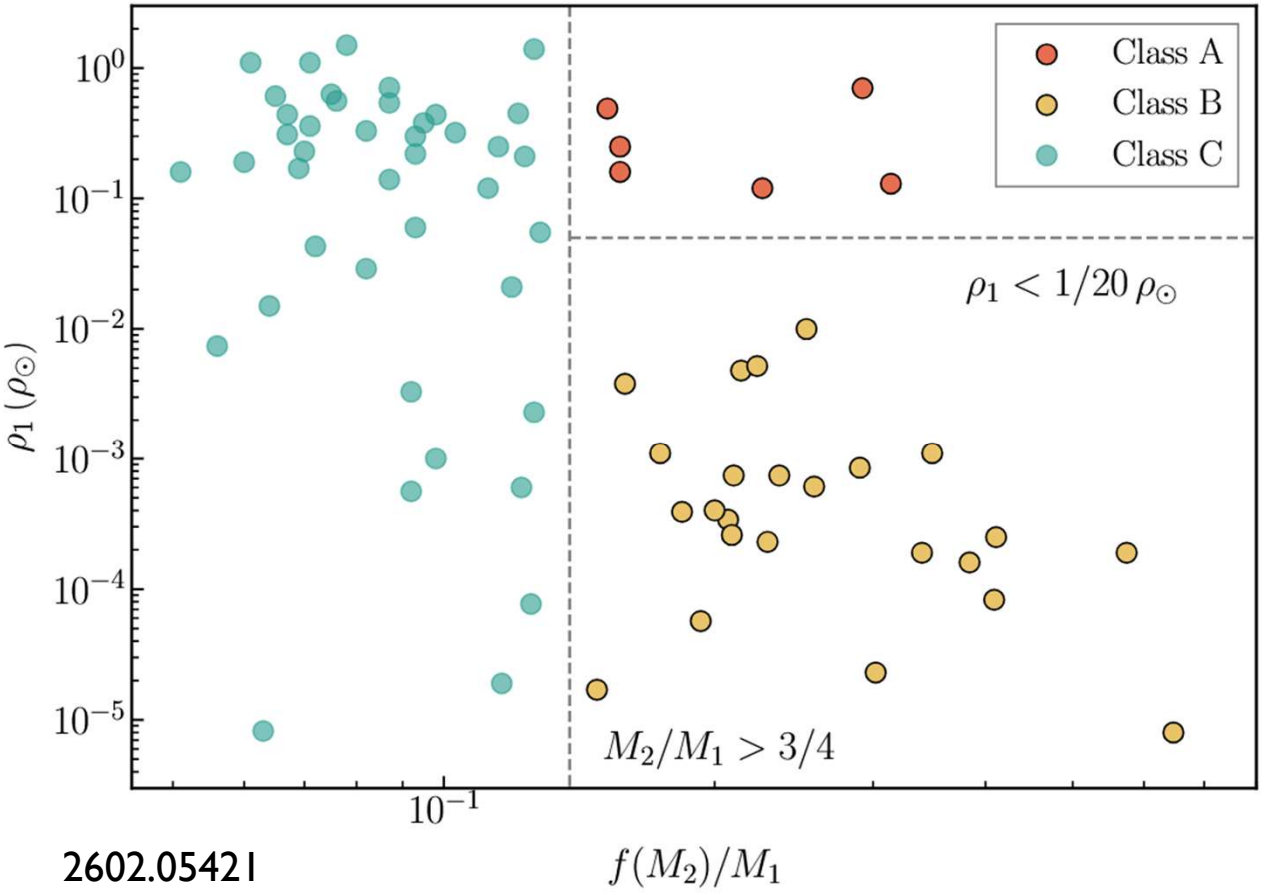

2602.05421

LAMOST Designation (J2000) (1)	$P_{\rm orb}$ (days) (4)	M_1 ($M_\odot$) (10)	$M_{2,\rm min}$ ($M_\odot$) (11)
J060228.6+280758.3	120.8	1.12	1.26
J084314.4+133049.9	1184.9	0.98	0.78
J084423.8+152520.8	448.2	1.00	0.95
J084437.0+194238.9	142.7	1.02	0.80
J084925.8+111656.9	114.9	0.64	0.51
J085354.6+112346.6	240.4	0.84	0.91

Candidates are based on LAMOST observations. Additionally, Gaia data is used in the analysis.

J0602 was also reported by Zhao et al. (2024).

COMPARISON WITH OTHER SYSTEMS

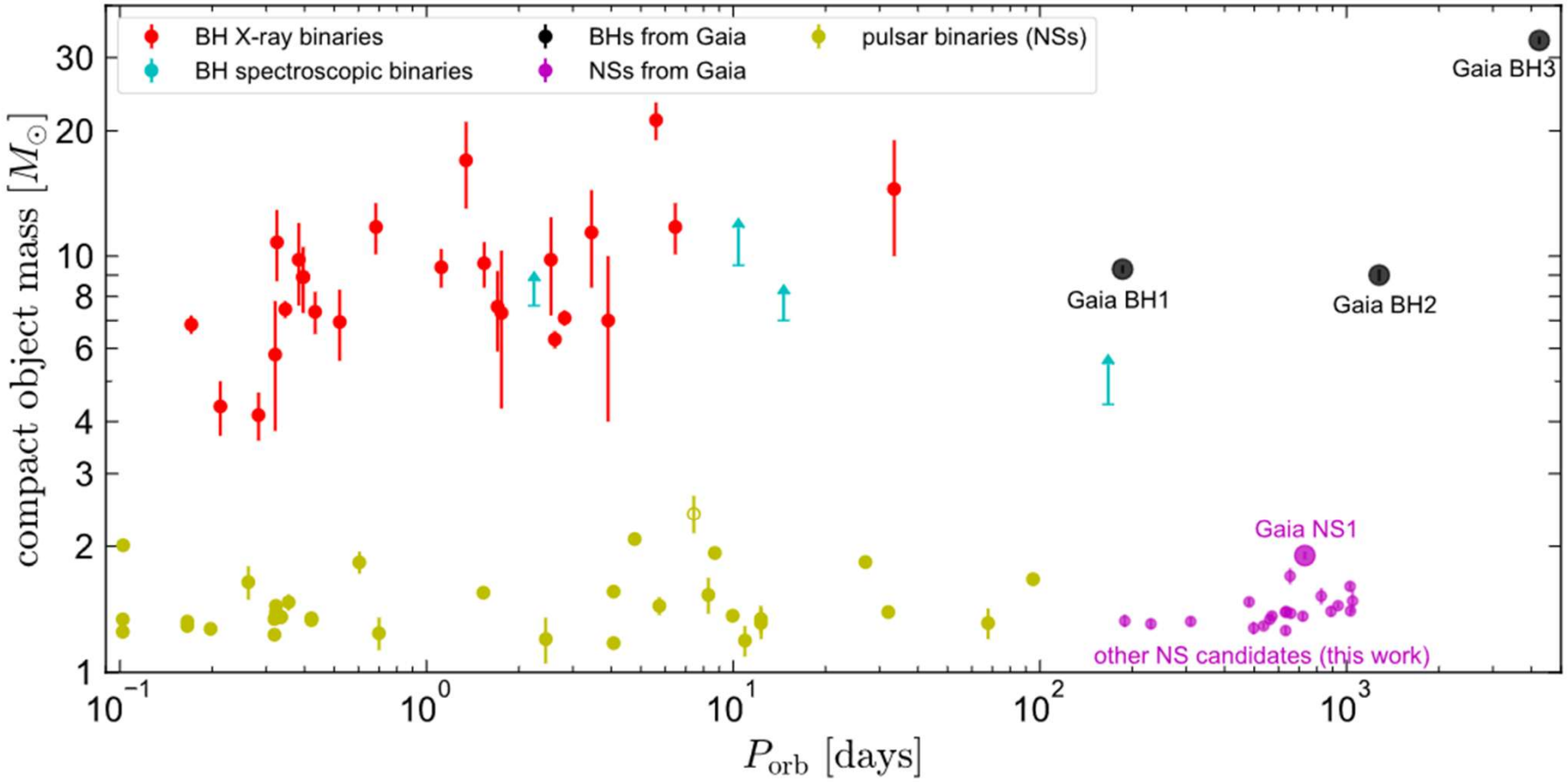

2405.00089

ORIGIN OF WIDE BINARIES WITH NSS. KICK PROPERTIES.

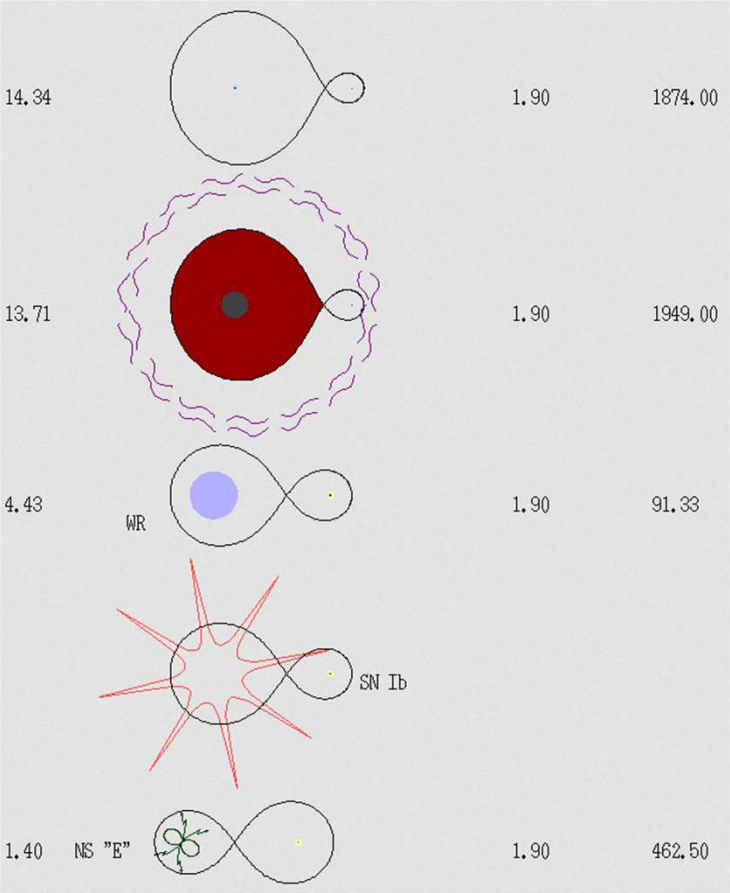

Formation of wide NS binaries with low-mass companions requires some special conditions.

E.g., in many cases the system can be destroyed due to the kick or/and mass loss by the NS's progenitor.

Systems are expected to have significant eccentricity after the NS formation.

https://xray.sai.msu.ru/sciwork/scenario.html

BSE-like code with accounting for the compact object evolution.

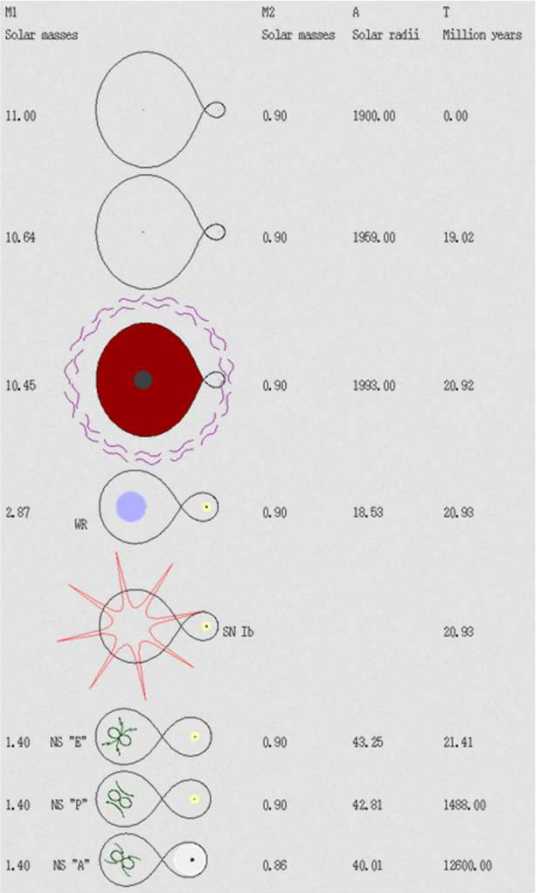

EVOLUTION NEUTRON STARS IN WIDE BINARIES

In many respects, evolution of NSs in wide low-mass binaries is similar to the evolution of isolated NSs (see 2402.04331) .

For billions of years, the evolution proceeds under a relatively constant conditions with a low-density (n <~ a few particles cm^{-3}) matter flow.

In the case of INSs, the density is the ISM density and the relative velocity is the spatial velocity due to the kick. In the case of wide binaries, the density and velocity are mainly determined by the stellar wind and the size of the orbit.

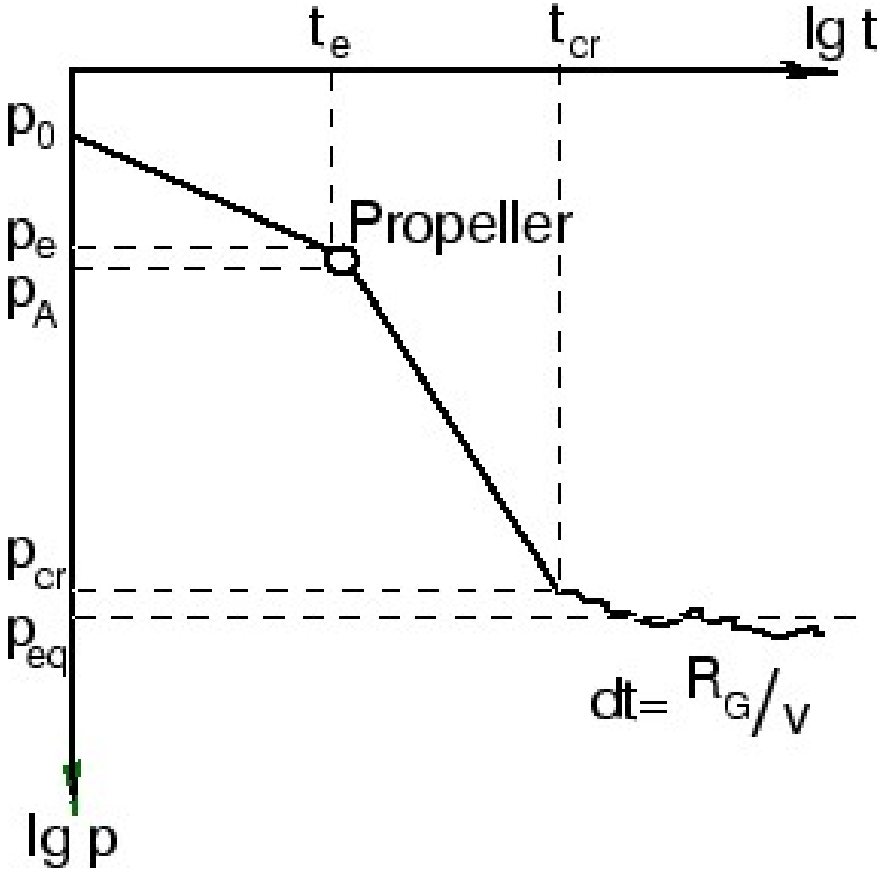

PROPERTIES OF THE MATTER FLOW

In our study, we use properties of the stellar wind which corresponds to a solar-like star along its history taken from Johnstone et al. (2015):

$$\dot{M}_{\rm w} = \dot{M}_{\rm w0}\left(\frac{t}{4.6\ {\rm Gyr}}\right)^{-0.75}$$

The stellar wind density is calculated as: $\rho(r) = \dfrac{\dot{M}_{\rm w}}{4\pi r^2 v_{\rm w}}$

The velocity is taken to be 400 km/s
and $c_{\rm s} \approx \sqrt{k_{\rm B}T/m_{\rm p}} \approx 30\ {\rm km\ s^{-1}}$

Also, the orbital velocity is important,
especially for eccentric orbits: $\vec{v} = \vec{v}_{\rm w} - \vec{v}_{\rm orb}$

In the plot on the right,
the age of a sun-like star is 4.6 Gyr,
the semi-major axis is a = 1 AU,
and the eccentricity is e = 0.6

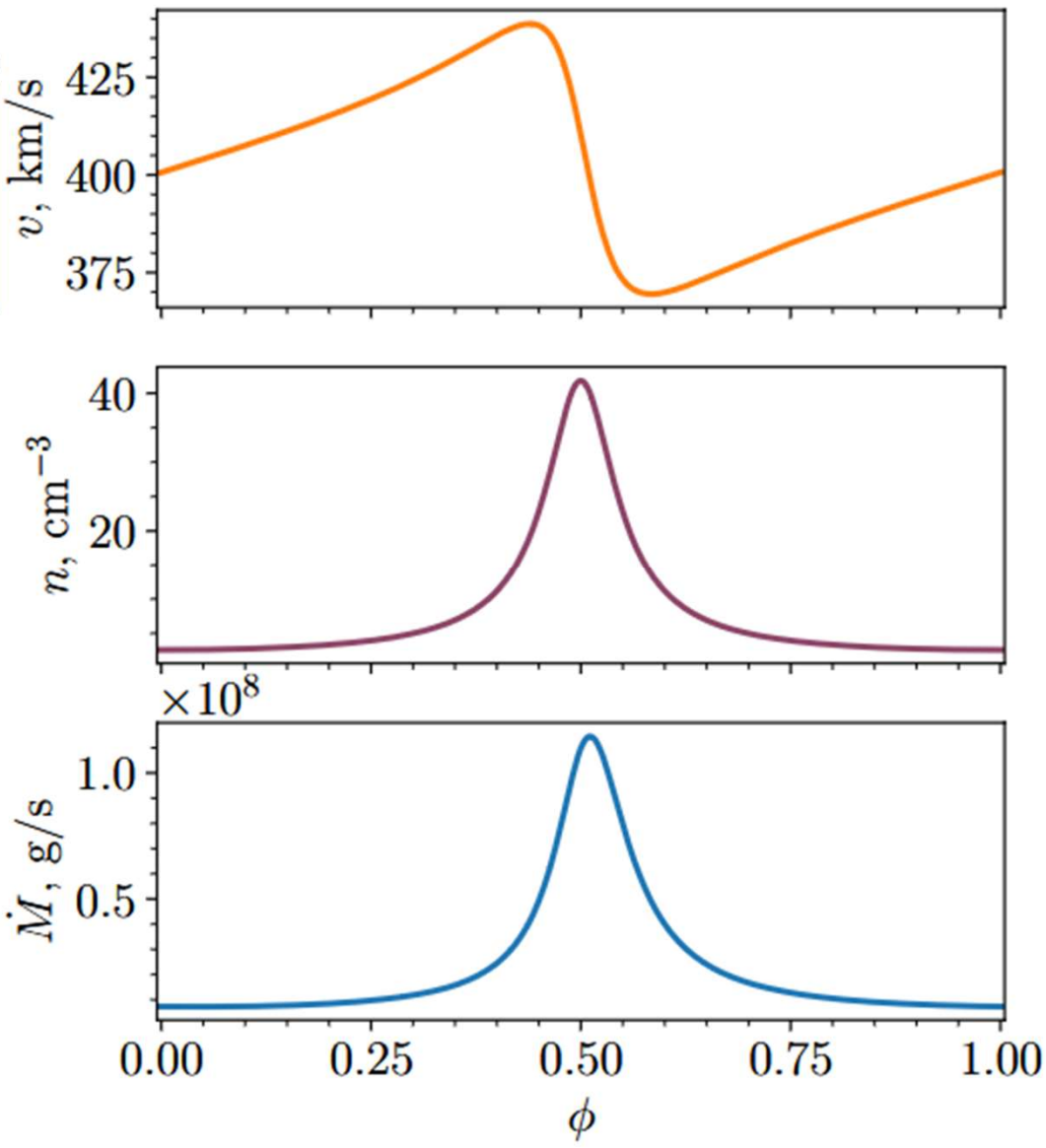

2501.15918

MAGNETO-ROTATIONAL EVOLUTION OF NEUTRON STARS

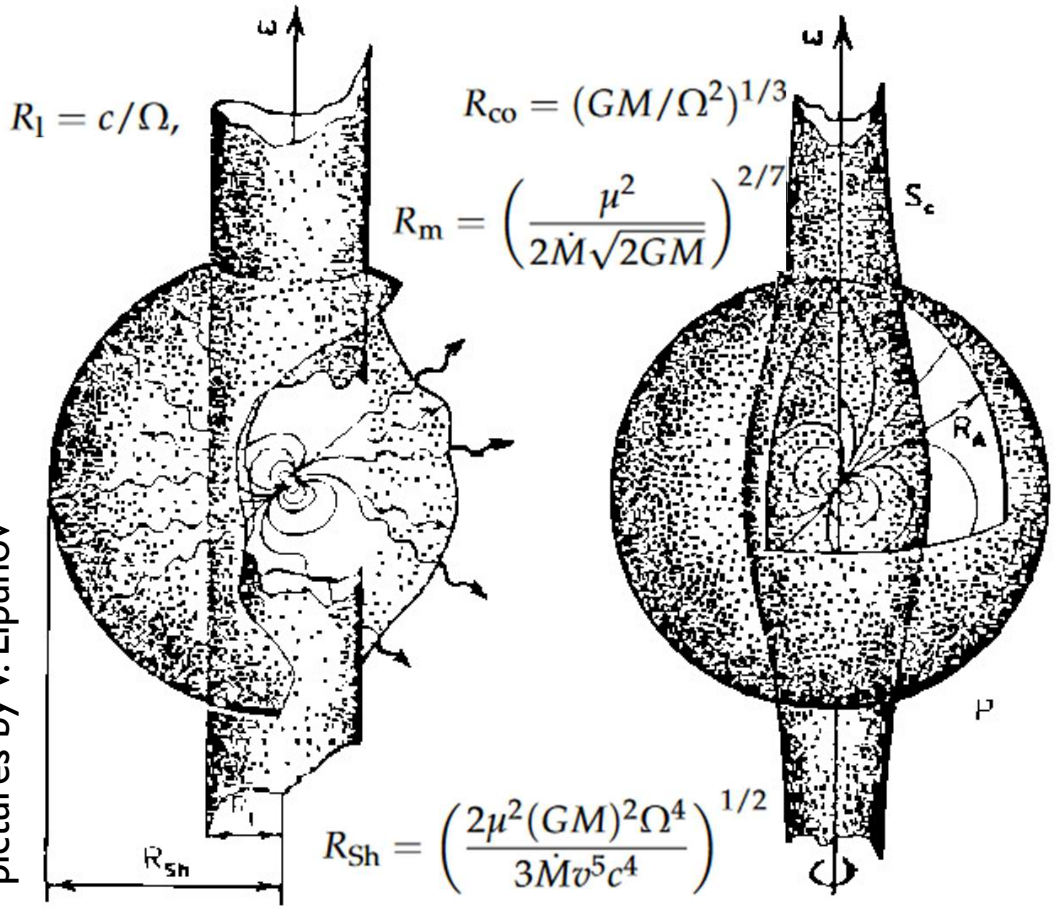

pictures by V. Lipunov

Typically, spinning down during its lifetime a NS passes through several consequent stages

Ejector → Propeller → Accretor

Stages can be described by relations between several critical radii.

Evolution of the magnetic field and variations in the external conditions can make the evolution more complicated.

Generally, we follow Lipunov (1992).

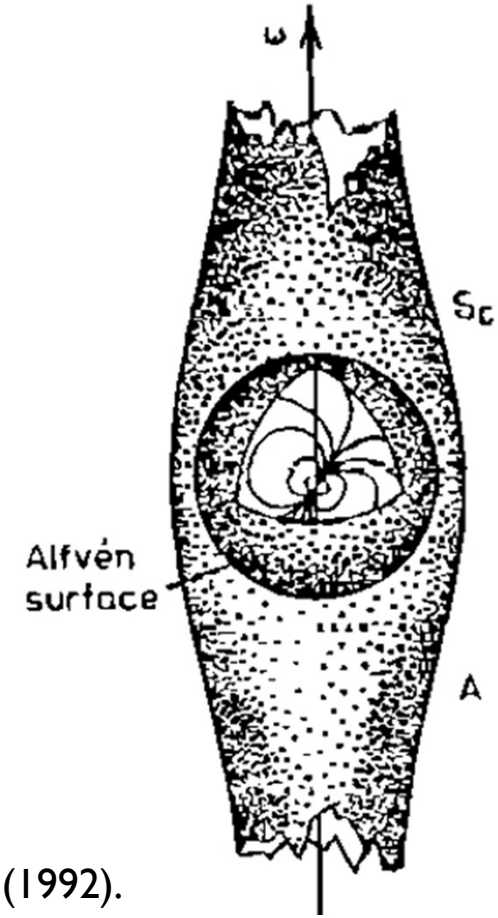

EVOLUTIONARY STAGES OF A NEUTRON STAR

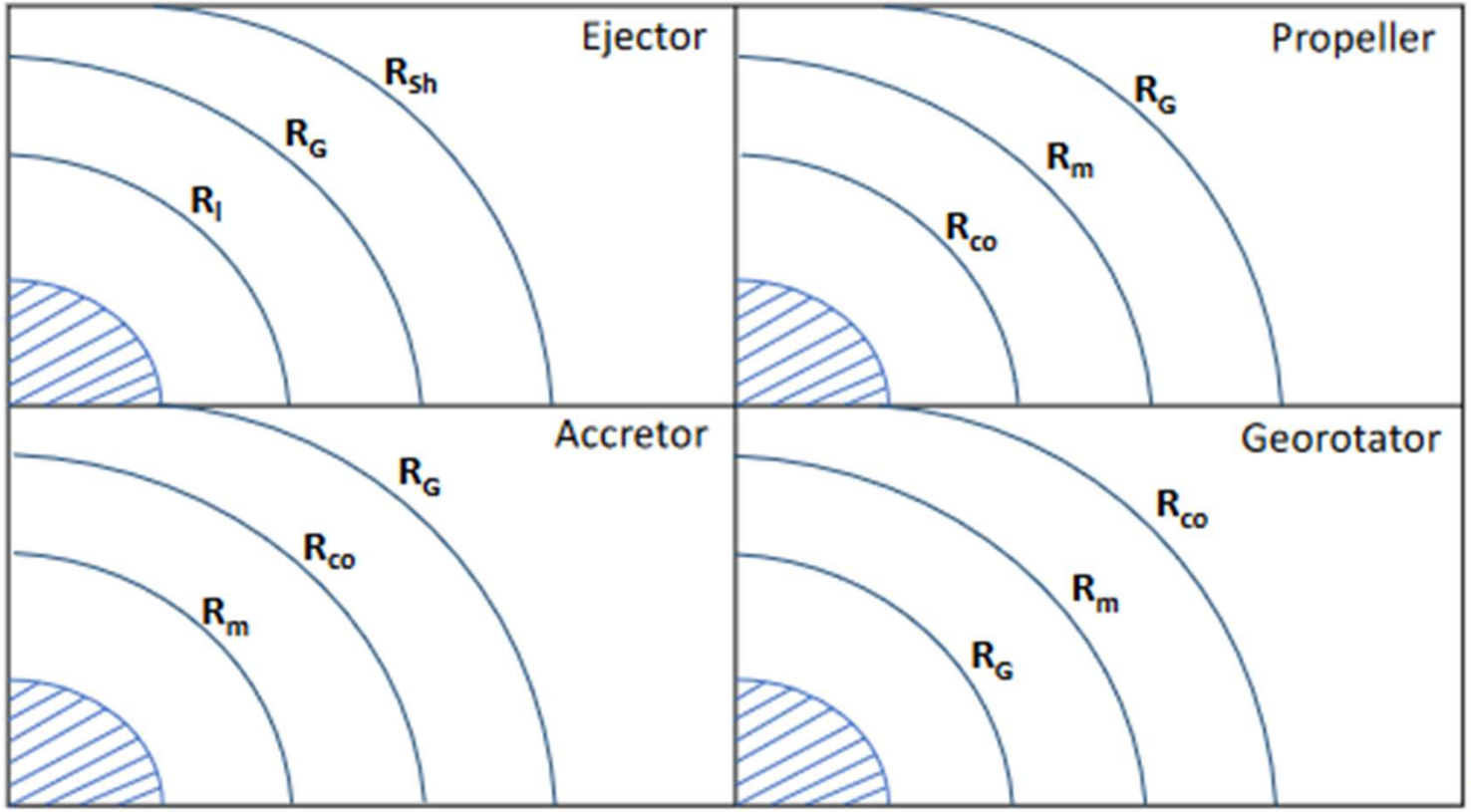

$R_G = \frac{2GM}{v^2}$ Bondi radius

Light cylinder $R_l = c/\Omega,$

$R_{co} = (GM/\Omega^2)^{1/3}$ Corotation

Shvartsman radius

$$R_{Sh} = \left(\frac{2\mu^2(GM)^2\Omega^4}{3\dot{M}v^5c^4}\right)^{1/2}$$

or $R_{Sh}^{env} = R_G\left(\frac{\xi\mu^2\omega^4}{c^4\dot{M}v_\infty}\right)^2$

$R_m = \left(\frac{\mu^2}{2\dot{M}\sqrt{2GM}}\right)^{2/7}$ Alfven radius

2402.04331

SPIN BEHAVIOR AT DIFFERENT STAGES

Ejector

$$I\frac{d\omega}{dt} = -K \qquad K_{\rm E} = 2\frac{\mu^2}{R_{\rm l}^3}$$

Transition to Propeller
at the critical period $P_{\rm EP}$:

$$P_{\rm EP} = \begin{cases} \frac{2\pi}{c}\left(\frac{2\mu^2}{4\dot{M}v}\right)^{1/4}, & R_{\rm G} > R_{\rm l} \\ \frac{2\pi}{c}\left(\frac{2\mu^2(GM)^2}{\dot{M}v^5}\right)^{1/6}, & R_{\rm G} \le R_{\rm l} \end{cases}$$

It corresponds to $R_{\rm Sh} = R_{\rm l}$

In addition, we consider the `transient ejector' stage.

Accretor

$$K_{\rm A} = K_{\rm sd} - K_{\rm su}$$

$$K_{\rm sd} = k_{\rm t}\frac{\mu^2}{R_{\rm co}^3} \quad \text{or} \quad K_{\rm sd} = k_{\rm t}\frac{\mu^2}{R_{\rm cb}^3}$$

$$R_{\rm cb} = 0.87R_{\rm co} = 0.87\left(\frac{GM}{\omega^2}\right)^{1/3}$$

(Lyutikov 2023)

$$K_{\rm su} = \begin{cases} \dot{M}\sqrt{GMR_{\rm A}}, & \text{disc} \\ \dot{M}\eta\Omega R_{\rm G}^2, & \text{no disc} \end{cases} \qquad K_{\rm su} = K_{\rm sd}$$

The spin equilibrium can be reached if

$$P_{\rm eq} = 2\pi\mu\sqrt{\frac{k_{\rm t}}{GMK_{\rm su}}}.$$

We also consider the exponential magnetic field decay $B = B_0\exp(-t/\tau_{\rm Ohm})$

PROPELLER REGIME

Propeller stage properties are very uncertain.
Several models have been proposed.

We use four approaches:

Model A: Shakura (1975)
Model B: Davidson, Ostriker (1973)
Model C: Illarionov, Sunyaev (1975)
Model D: Davies, Pringle (1981)

Model A provides the fastest spin-down.

Spin-down rates within models C and D
are too slow to allow an NS to start accreting
in a wide low-mass binary.

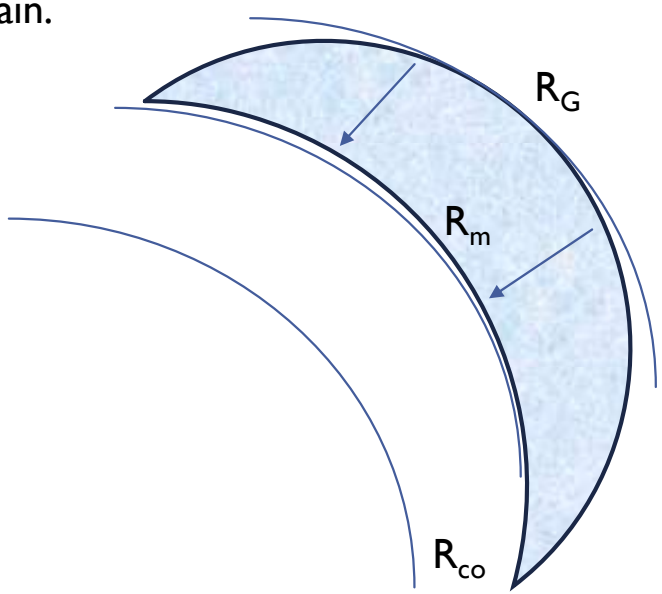

Matter cannot penetrate
inside the magnetosphere
while the NS is rapidly rotating
and plasma is hot.

$$I\frac{d\omega}{dt} = -K$$

Model	Braking torque K
A	$\dot{M}\omega R_m^2$
B	$\dot{M}\sqrt{2GMR_m}$
C	$\dot{M}\max(v_\infty^2,\ v_{ff}^2(R_m))/(2\omega)$
D	$\dot{M}v_\infty^2/(2\omega)$

At this stage,
the magnetospheric radius
is defined as: $R_A^{7/9}R_G^{2/9}$

2501.15918

NEUTRON STAR EVOLUTION IN A CIRCULAR ORBIT. I.

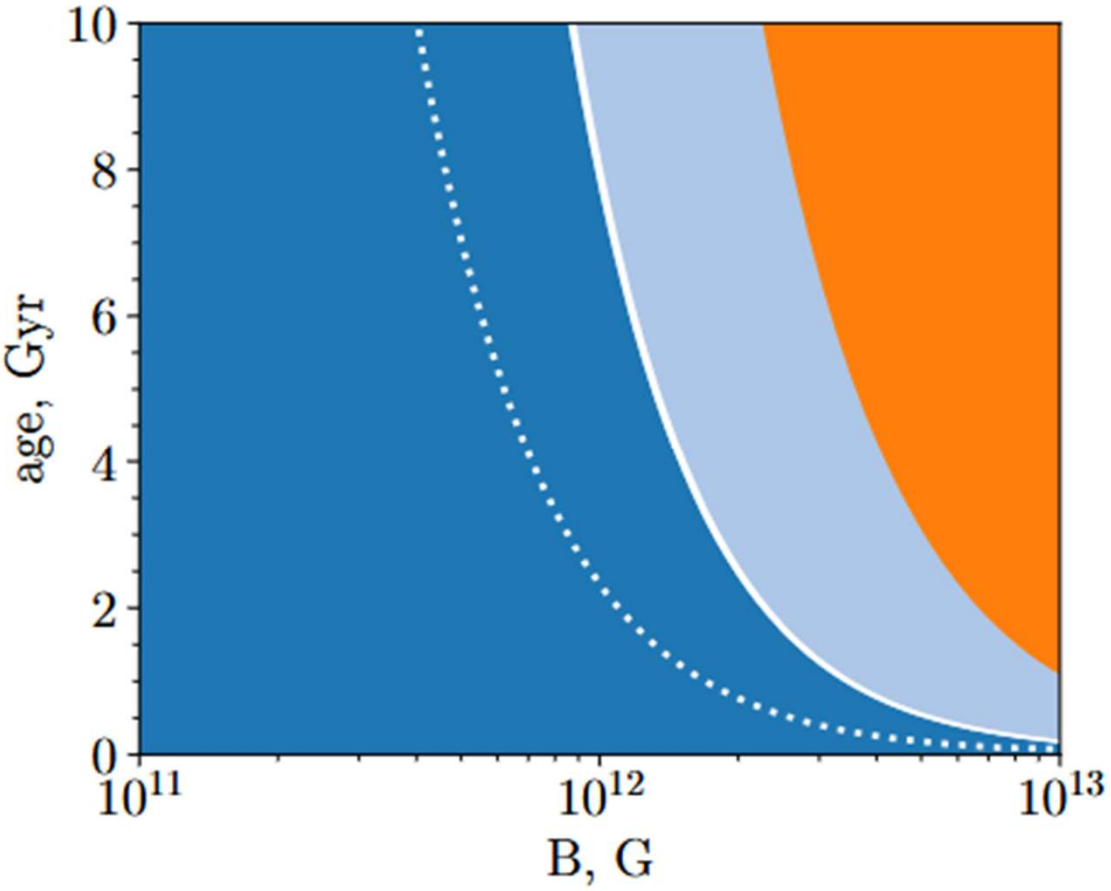

The evolutionary stages of NS with a constant magnetic field B in a circular orbit with semi-major axis a = 1 AU at a given age.

The ejector stage is dark blue.

The dotted line shows the transition to the TE stage.

The short propeller stage in model A is shown in white. For model B, the propeller stage is both the white and light blue regions.

The rest of the plot is the accretor stage: the light blue and orange areas in model A and orange in model B.

2409.00714

NEUTRON STAR EVOLUTION IN A CIRCULAR ORBIT. II.

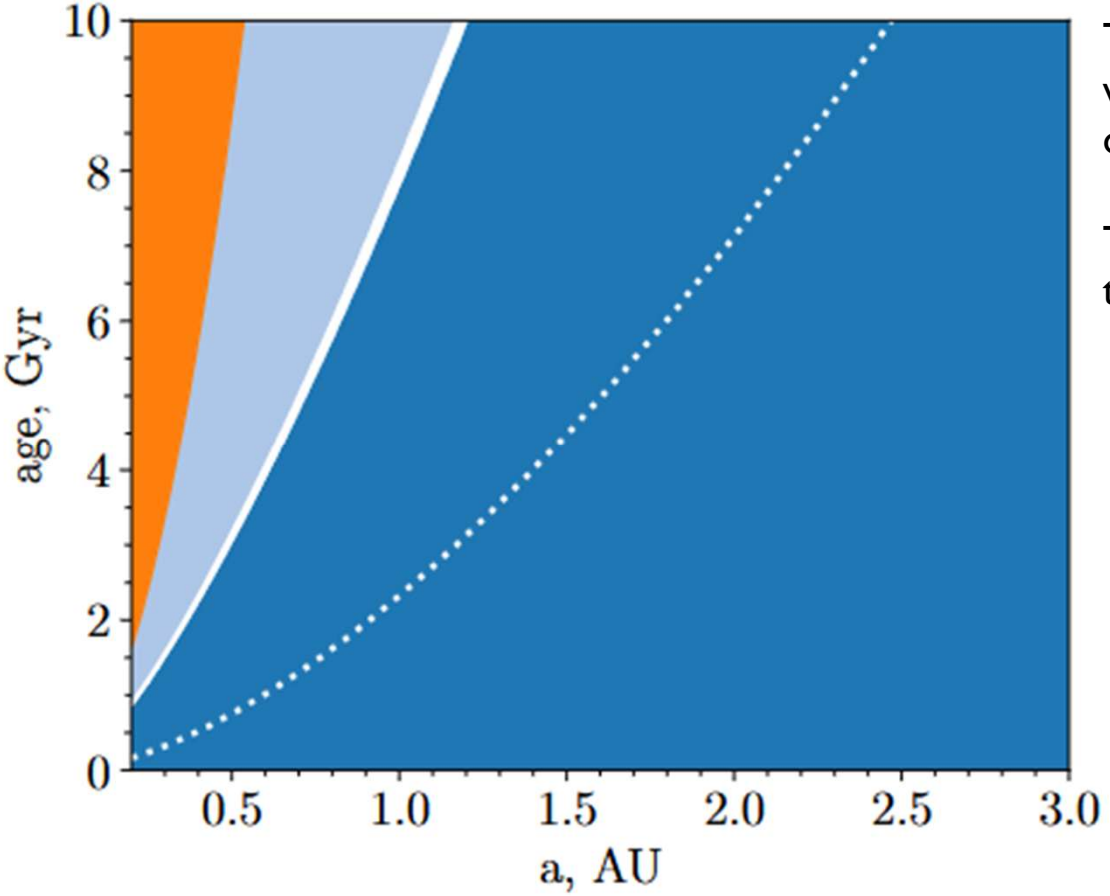

The evolution of an NS
with the constant magnetic field $B = 10^{12}$ G
on a circular orbit with the semi-major axis a.

The colors and the white dotted line represent
the evolutionary stages for the propeller models A and B.

2409.00714

EVOLUTION IN AN ECCENTRIC ORBIT. I.

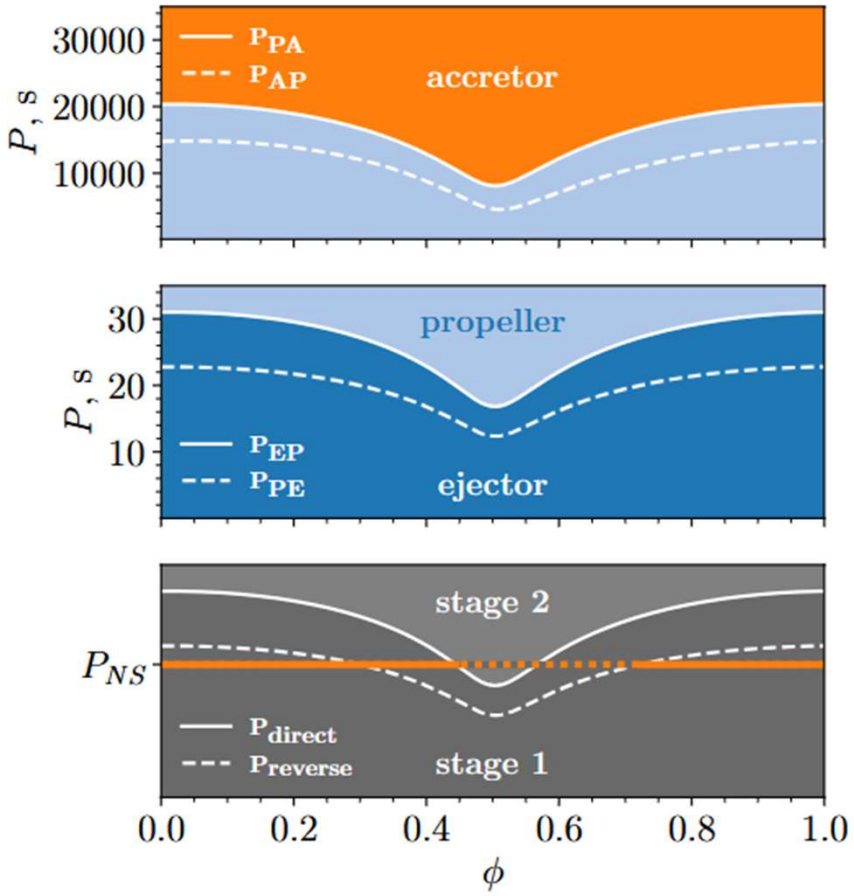

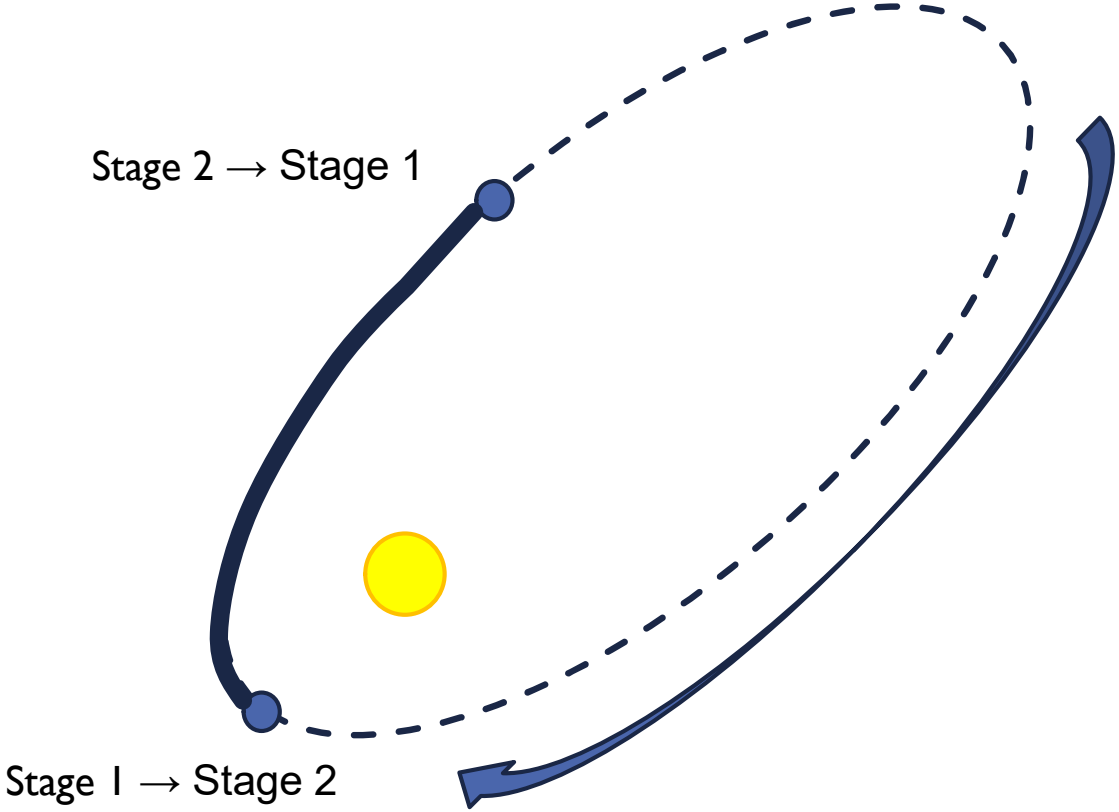

2501.15918

AVERAGE ACCRETION RATE

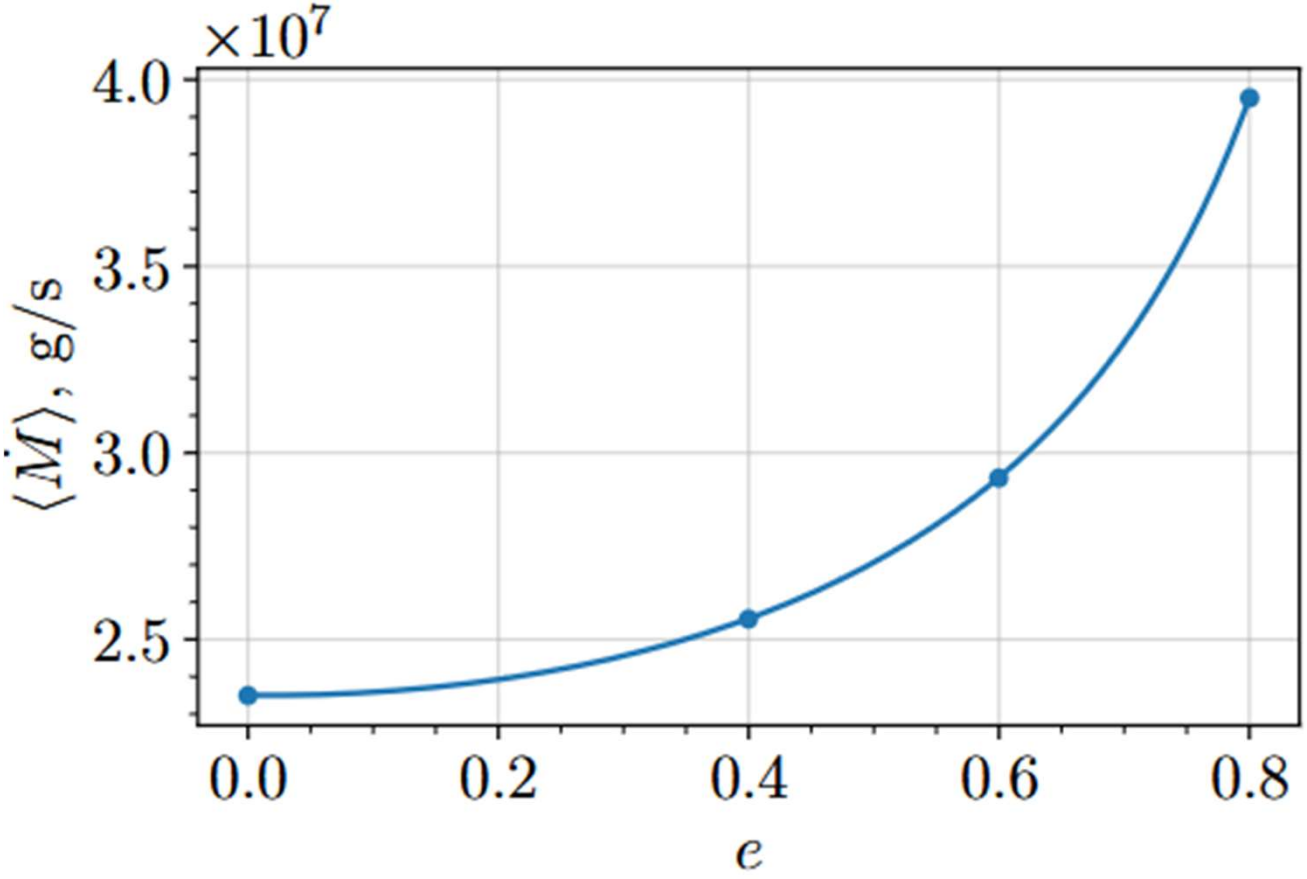

The orbit-averaged accretion rate of the NS in the orbit with an eccentricity e.

The dots highlight the eccentricities we consider for the evolution of NSs.

The parameters of the Sun-like star correspond to an age of the Sun 4.6 Gyr.

$$\langle \dot{M} \rangle = \int_0^1 \dot{M}(\phi) \mathrm{d}\phi$$

2501.15918

VERY RAPID PROPELLER SPIN-DOWN. MODEL A. $B_0=10^{12}$ G

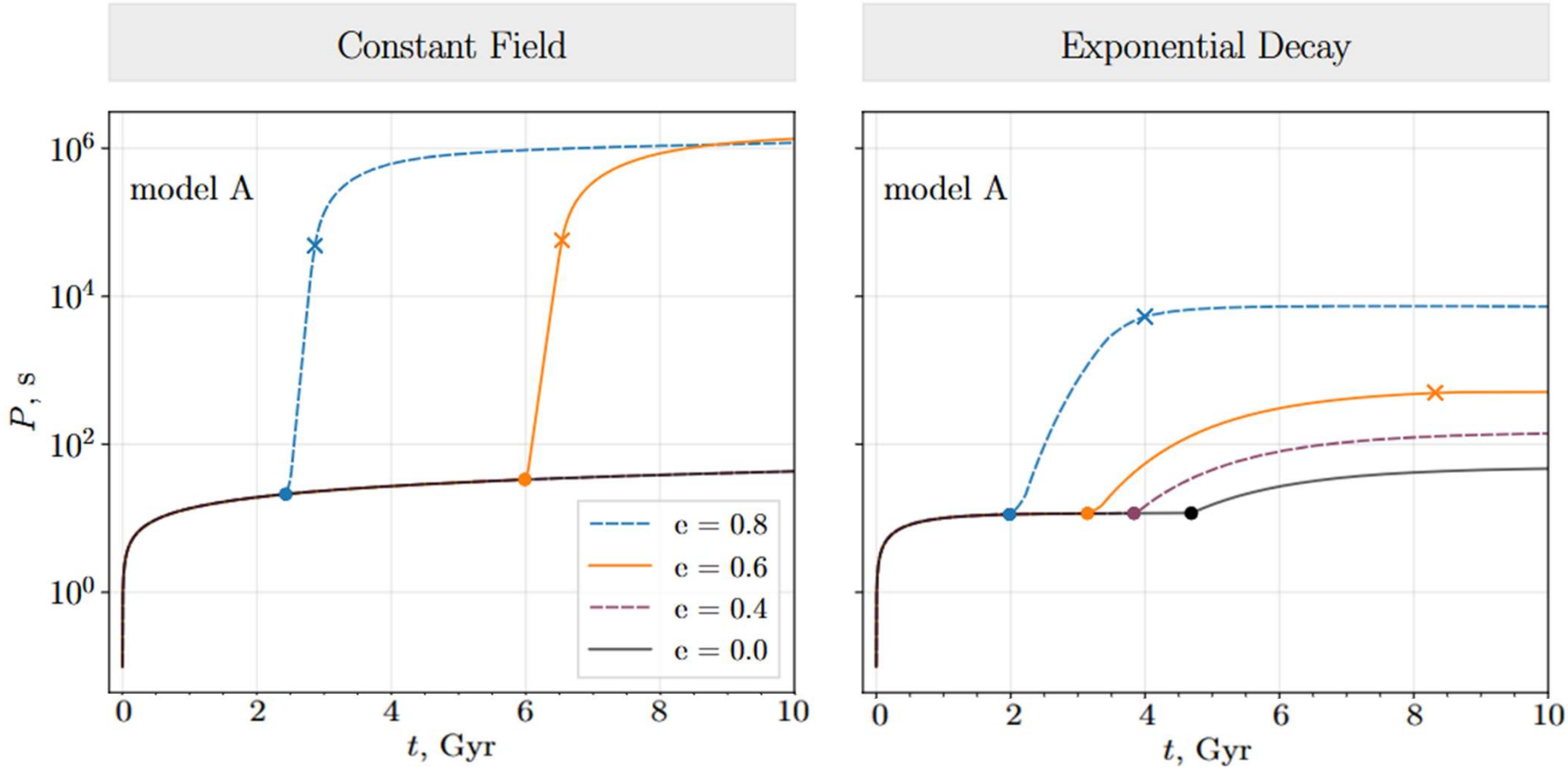

2501.15918

RAPID PROPELLER SPIN-DOWN. MODEL B. $B_0=10^{12}$ G

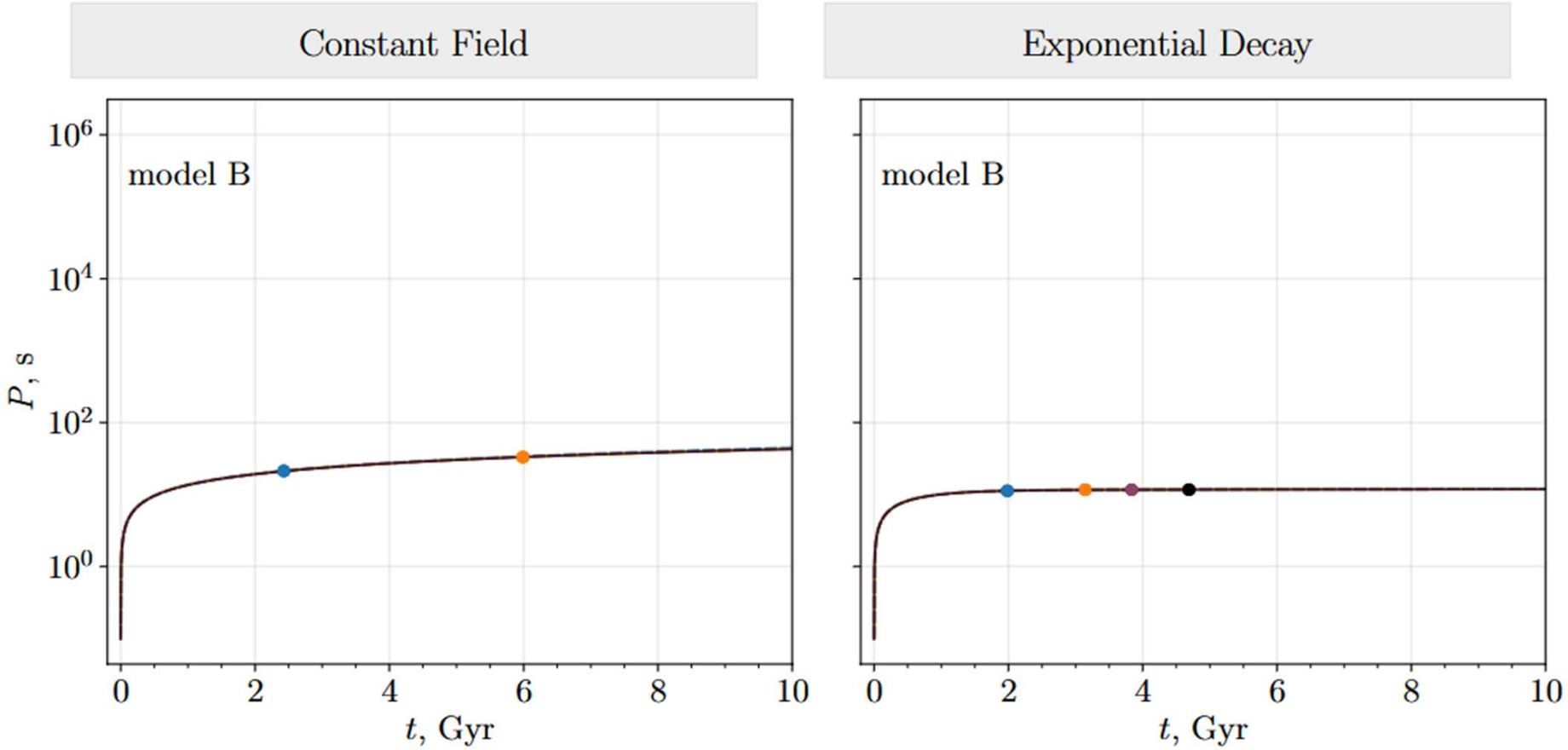

2501.15918

HIGHER FIELD. MODEL A. $B_0 = 10^{13}$ G

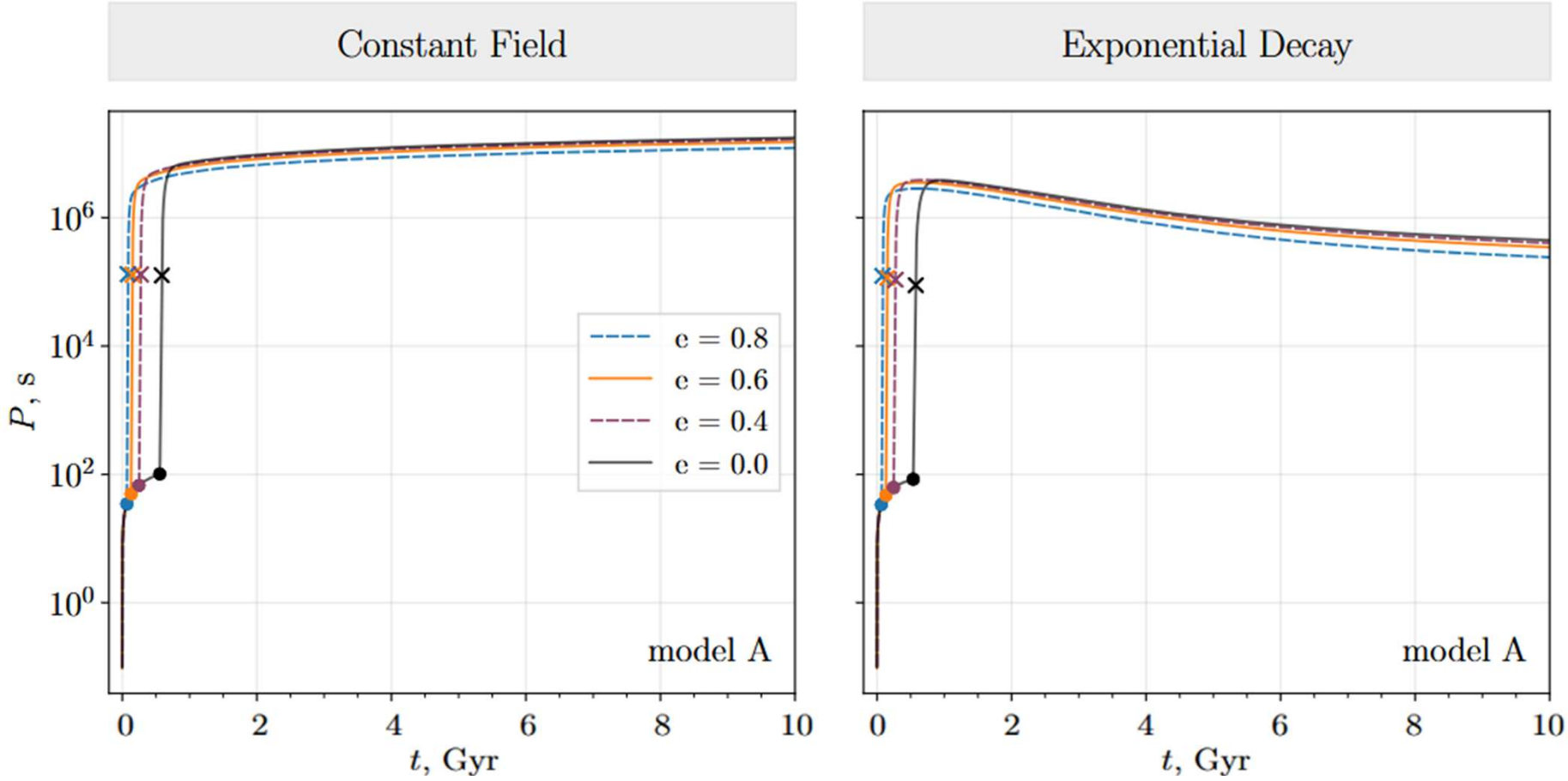

2501.15918

HIGHER FIELD. MODEL B. $B_0 = 10^{13}$ G

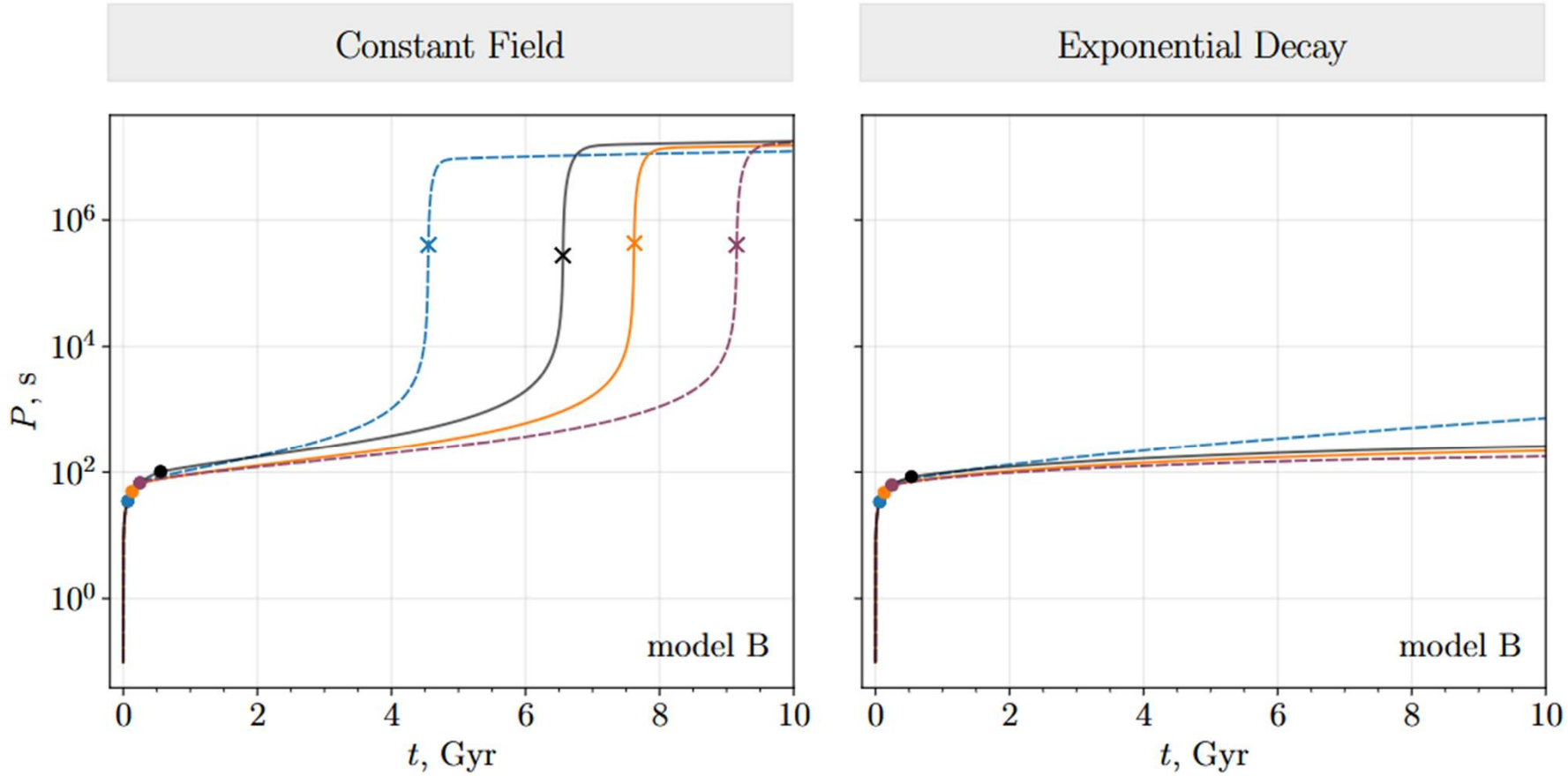

2501.15918

RELATIVE DURATION OF VARIOUS EVOLUTIONARY STAGES

B	10^{12} G				10^{13} G			
e	0	0.4	0.6	0.8	0	0.4	0.6	0.8
E_A	1.00	1.00	0.61	0.26	0.06	0.03	0.02	0.01
P_A	0.00	0.00	0.06	0.04	0.01	0.01	0.01	0.01
A_A	0.00	0.00	0.34	0.70	0.93	0.97	0.98	0.98
E_B	1.00	1.00	0.92	0.89	0.06	0.03	0.03	0.02
P_B	0.00	0.00	0.08	0.11	0.61	0.88	0.74	0.44
A_B	0.00	0.00	0.00	0.00	0.34	0.09	0.24	0.54

2501.15918

Constant field

EFFECT OF THE ACCRETION RATE VARIATION

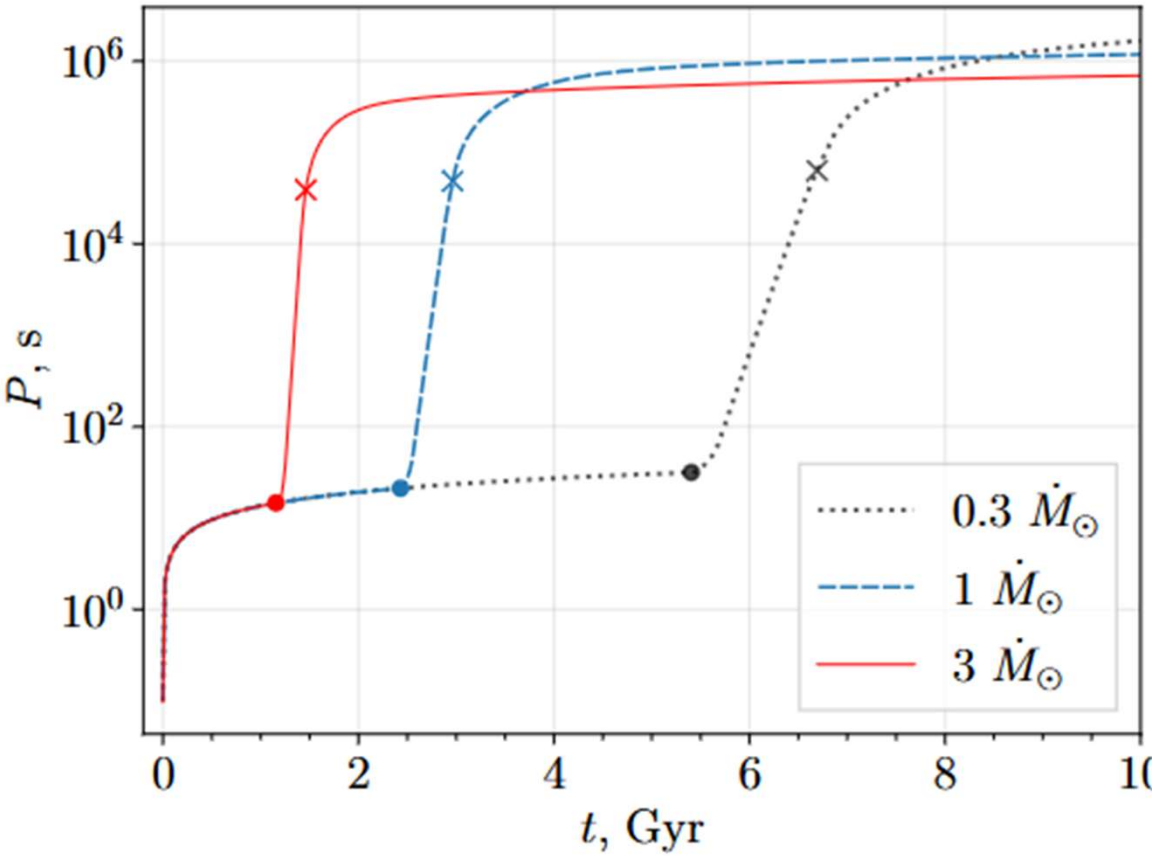

The spin evolution of the NS
with the constant magnetic field B = 10^{12} G,
e = 0.8, a = 1 AU in the case of the propeller model A.

The lines are plotted for three values
of the accretion rate which is given in units
of the rate corresponding to the Sun as the donor.

$\dot{M}_w \propto R_*^2 M_*^{-3.36} \Omega_*^{1.33}$ Johnstone et al. (2015)

Still, variation of the semi-major axis might be
more important than variations of the stellar mass,
metallicity, etc.

2501.15918

OBSERVABILITY

Ejector

NS wind has power ~10^{27}-10^{28} erg/s.
The MS wind is less powerful.

Propeller

$$L_{\rm prop} = \frac{GM}{R_{\rm m}}\dot{M} \approx 10^{23}\dot{M}_8\left(\frac{M}{M_\odot}\right)\left(\frac{R_{\rm m}}{10^{11}\,{\rm cm}}\right)^{-1}\ {\rm erg\ s^{-1}}$$

There is not much hope to discover emission from the NS companions. Still, it is worth trying.

Accretor

$$L = \frac{GM}{R_{\rm NS}}\dot{M} \approx 10^{28}\dot{M}_8\left(\frac{M}{M_\odot}\right)\left(\frac{R_{\rm NS}}{10^{6}\,{\rm cm}}\right)^{-1}\ {\rm erg\ s^{-1}}$$

This is an upper limit for a persistent source.

RADIO OBSERVATIONS

System	Distance, pc	P_{orb}, d	Eccentricity	M_*, $M_\odot$	Ref.
J0616+2319	1111	0.8666	≈ 0	1.7	Sbarufatti et al. (2024)
J1527+3536	118	0.2557	≈ 0	0.62	Sbarufatti et al. (2024)
J2102+3703	657	481.04	0.45	1.03	El-Badry et al. (2024)
J2128+3316	227	1430	0.59	0.7	Sbarufatti et al. (2024)
J2145+2837	242	889.5	0.58	0.95	El-Badry et al. (2024)

Pushchino LPA

Archival data: August 16, 2014, to June 15, 2025 (3956 days).

111 MHz (2.5 MHz bandwidth)

No persistent sources found.

One strong burst (and several weaker candidates) are detected from J1527.

THE BURST FROM J1527+3536. 13 JY

2509.03001

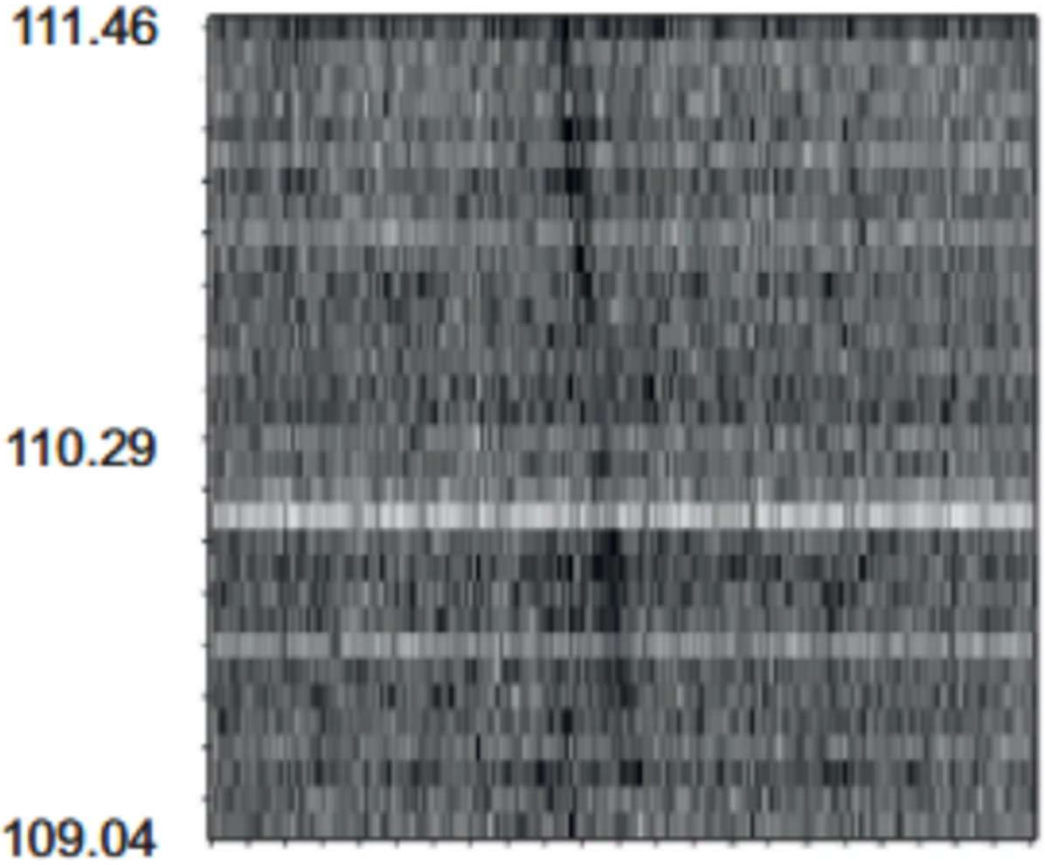

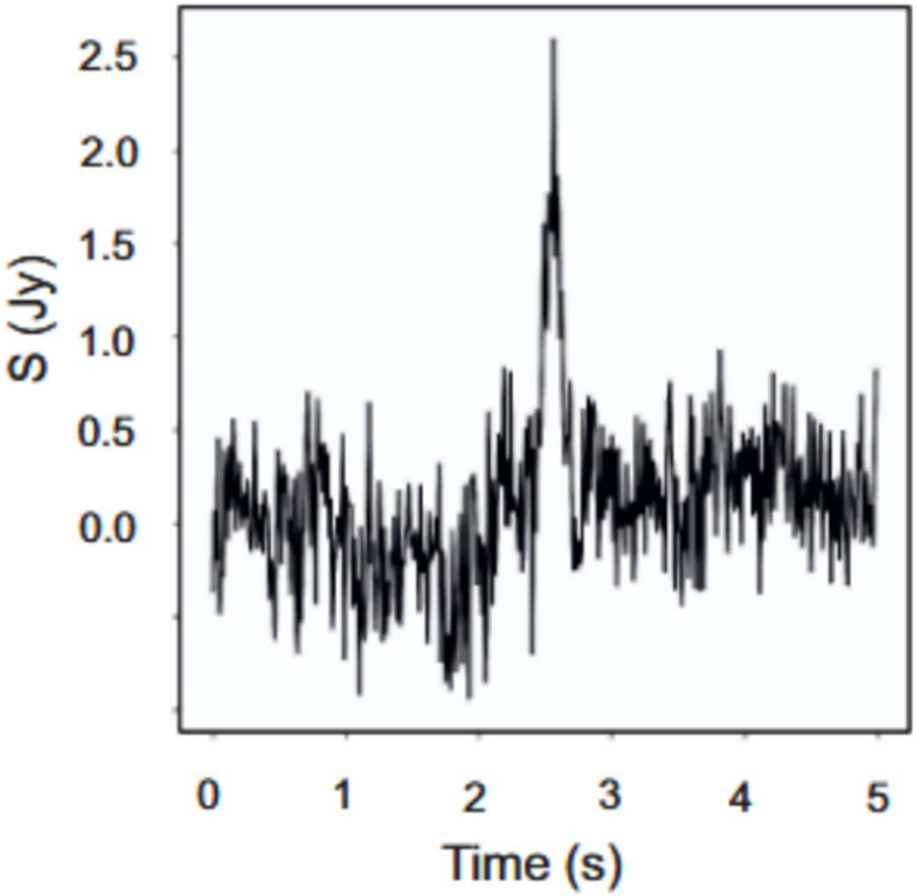

POSSIBLE INTERPRETATION

2509.03001

Object	$P_{\rm pulse}$, m	$P_{\rm spin}$, s	$P_{\rm orb}$, h	Δt, s	$L_{\rm radio}$, erg s^{-1}	M_*, $M_\odot$	Ref.
J1527+3536	—	—	6.14	0.13	5.6×10^{26}	0.62	Lin et al. (2023) and this work
GLEAM-X J0704-37	175	—	2.9	~ 30	~ 10^{26}	0.14	Hurley-Walker et al. (2024)
ILT J1101 + 5521	125.5	7530 (?)	2.1	~ (30-90)	~ 10^{27}-10^{28}	≈ 0.2	de Ruiter et al. (2025)
AR Sco	1.97	117	3.56	~ 100	~ 10^{27}	≈ 0.3	Marsh et al. (2016)
J1912-4410	5.3	319	4.03	$\lesssim 4$	$\approx 10^{27}$	≈ 0.3	Pelisoli et al. (2023)
AE Aqr	0.55	33	9.9	~ 10	8×10^{25}	~ 0.6	Madzime et al. (2022)
J024048.51+195226.9	—	—	7.3	—	~ 2.5×10^{26}	~ 0.5	Pretorius et al. (2021)
J230641.47+244055.8	—	92	3.49	—	—	0.19-0.28	Castro Segura et al. (2025)

The system, most probably, contains a WD as a compact object (Zhang et al. 2024, Lin et al. 2023).
Thus, the sources can be in some respects similar to LPRTs.
We exclude a background extragalactic source, a stellar flare, and a burst from an NS (including sources in the halo).

SHORT-PERIOD NON-INTERACTING BINARIES WITH INVISIBLE MASSIVE COMPANIONS

LAMOST observations allowed for discovering several candidates for short-period low-mass binaries with massive invisible companions, which can be WDs or NSs.

	$P_{\rm orb}$ (days)	Distance (pc)	M_2 ($M_\odot$)
J0341	1.10	276±2	$1.39^{+0.09}_{-0.10}$
J0359	1.38	1061±17	$1.34^{+0.08}_{-0.09}$
J2354	0.48	127±1	$1.34^{+0.05}_{-0.07}$

Potentially, there might be a large population of NSs in low-mass non-interacting binaries with orbital periods <~a few days.

Many of them can become accretors with Mdot ~ 10^{10}-10^{13} g/s as rapidly rotating low-mass stars can provide stronger wind.

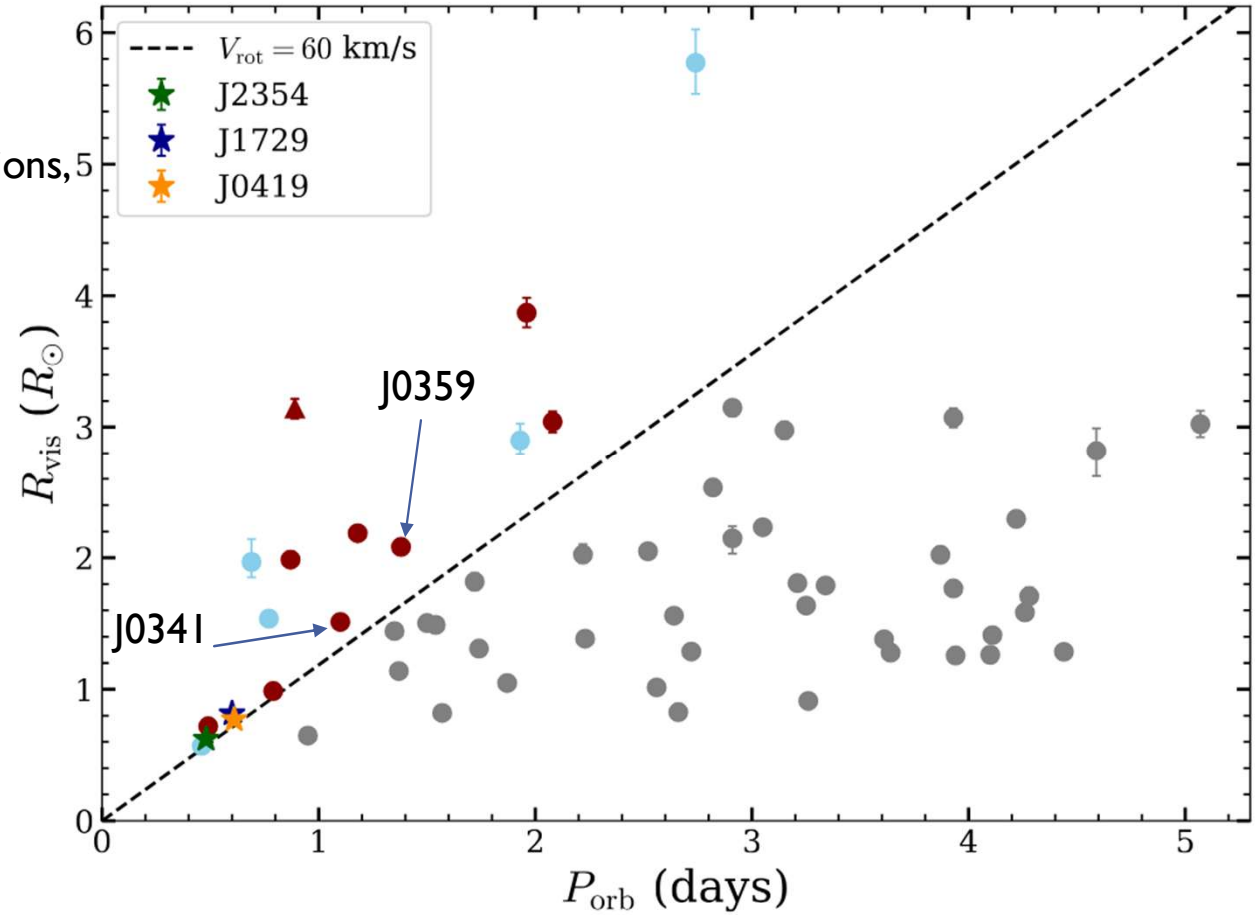

2603.09210

HIGH-VELOCITY X-RAY SOURCES

X-ray ID	F_X (10^{-14} erg cm^{-2} s$^-$	d_{b21} (kpc)
(1)	(5)	(7)
1eRASS J003051.3−370912	6.9 ± 2.9	$3.0^{+0.5}_{-0.4}$
1eRASS J015648.6−224326	6.8 ± 2.2	$0.9^{+0.2}_{-0.2}$
1eRASS J025910.8−390331	3.0 ± 1.3	$1.7^{+0.1}_{-0.1}$
1eRASS J043509.3−481751	4.0 ± 1.0	$3.3^{+0.5}_{-0.5}$
1eRASS J082815.9+383457	8.5 ± 3.6	$0.60^{+0.02}_{-0.02}$
1eRASS J142449.5−153938	3.6 ± 1.5	$1.2^{+0.1}_{-0.1}$
1eRASS J152027.0−030609	7.4 ± 2.8	$3.8^{+0.4}_{-0.4}$

Sources have luminosities ~a few 10^{30}-10^{33} erg/s

We suggest that some of them can be low-mass short-period non-interacting tidally synchronized binaries with NSs accreting from the stellar wind.

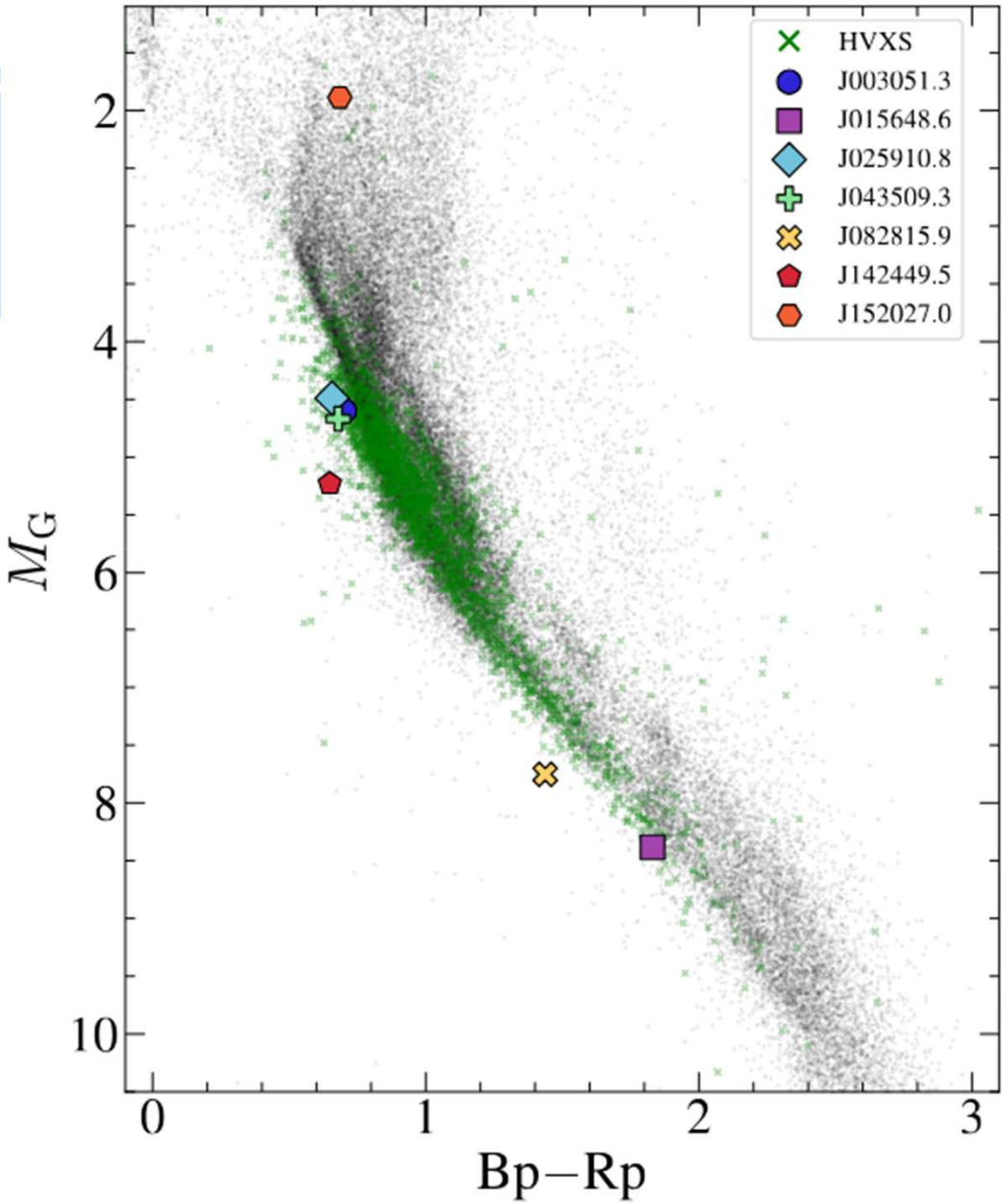

2601.02287

EXAMPLE OF THE BINARY EVOLUTION. BSE

TIME	M1	M2	K1	K2	SEP	ECC	R1/ROL1	R2/ROL2	TYPE
0.0000	12.500	0.600	1	0	951.614	0.00	0.007	0.004	INITIAL
16.7065	12.239	0.600	2	0	970.944	0.00	0.018	0.003	KW CHNGE
16.7454	12.235	0.600	3	0	971.269	0.00	0.461	0.003	KW CHNGE
16.7484	12.233	0.600	4	0	854.382	0.00	0.990	0.004	KW CHNGE
18.6579	11.412	0.601	5	0	908.900	0.00	0.941	0.004	KW CHNGE
18.6581	11.412	0.601	5	0	855.860	0.00	1.000	0.004	BEG RCHE
18.6581	3.787	0.601	8	0	13.761	0.00	1.000	0.004	COMENV
18.6581	3.787	0.601	7	0	13.761	0.00	0.069	0.172	KW CHNGE
18.6581	3.787	0.601	7	0	13.761	0.00	0.069	0.172	END RCHE
18.6581	3.787	0.601	8	0	13.761	0.00	0.069	0.172	KW CHNGE
18.7814	1.361	0.601	13	0	12.194	0.24	0.000	0.147	KW CHNGE
18.7814	1.361	0.601	13	0	12.187	0.24	0.000	0.147	BEG SYMB
15000.0000	1.361	0.601	13	0	11.967	0.21	0.000	0.156	MAX TIME

OUTLOOK

- Multiwavelength observations:

  - Archive digging
  - Deep observations
  - Monitoring for possible transient activity

- Population synthesis:

  - distribution of NS over stages
  - accounting for evolution before NS formation
  - various parameters of MS stars and orbits

- More detailed description of magnetic field evolution and spin behavior

- More systems!

CONCLUSIONS

- Several low-mass binary systems with an invisible NS companion have been identified in the Gaia and LAMOST data.
- We studied magneto-rotational evolution of NSs in circular and eccentric orbits with a=1 AU around a Sun-like star.
- We focus on the time spent by the NS in various stages: Ejector, Propeller, and Accretor for various initial magnetic fields and field evolution (constant and exponentially decaying).
- We use four models of spin-down in the Propeller stage.
- It is shown that for ineffective propellers, such NSs never start to accrete.
- For the rapid spin-down (Shakura 1975) NSs easily reach the stage of accretion within a few Gyr.
- Recently identified high-velocity X-ray sources can be wind-fed accreting NSs in low-mass binaries.